MNRAS 000, 1–18 (2022) Preprint 10 August 2022 Compiled using MNRAS LATEX style file v3.0

RR Lyrae From Binary Evolution: Abundant, Young and Metal-Rich

Alexey Bobrick[1]★, Giuliano Iorio[2,3,4]†, Vasily Belokurov[5,6], Joris Vos[7], Maja Vučković[8], Nicola Giacobbo[9]

[1]Technion - Israel Institute of Technology, Physics Department, Haifa, Israel 32000
[2]Dipartimento di Fisica e Astronomia "Galileo Galilei", Università di Padova, vicolo dell'Osservatorio 3, IT-35122, Padova, Italy
[3]INAF - Osservatorio Astronomico di Padova, vicolo dell'Osservatorio 5, IT-35122 Padova, Italy dell'Osservatorio 3, IT-35122, Padova, Italy
[4]INFN - Padova, Via Marzolo 8, I–35131 Padova, Italy
[5]Institute of Astronomy, University of Cambridge, Madingley Road, Cambridge CB3 0HA, UK
[6]Center for Computational Astrophysics, Flatiron Institute, 162 5th Avenue, New York, NY 10010, USA
[7]Astronomical Institute of the Czech Academy of Sciences, CZ-25165, Ondřejov, Czech Republic
[8]Instituto de Física y Astronomía, Universidad de Valparaíso, Gran Bretaña 1111, Playa Ancha, Valparaíso 2360102, Chile
[9]School of Physics and Astronomy & Institute for Gravitational Wave Astronomy, University of Birmingham, Birmingham, B15 2TT, UK

Accepted XXX. Received YYY; in original form ZZZ

ABSTRACT

RR Lyrae are a well-known class of pulsating horizontal branch stars widely used as tracers of old, metal-poor stellar populations. However, mounting observational evidence shows that a significant fraction of these stars may be young and metal-rich. Here, through detailed binary stellar evolution modelling, we show that all such metal-rich RR Lyrae can be naturally produced through binary interactions. Binary companions of such RR Lyrae partly strip their progenitor's envelopes during a preceding red giant phase. As a result, stripped horizontal branch stars become bluer compared to their isolated stellar evolution counterparts and thus end up in the instability strip. In contrast, in the single evolution scenario, the stars can attain such colours only at large age and low metallicity. While RR Lyrae from binary evolution generally can have any ages and metallicities, the Galactic population is relatively young (1 – 9 Gyr) and dominated by the Thin Disc and the Bulge. We show that Galactic RR Lyrae from binary evolution are produced at rates compatible with the observed metal-rich population and have consistent G-band magnitudes, Galactic kinematics and pulsation properties. Furthermore, these systems dominate the RR Lyrae population in the Solar Neighbourhood. We predict that all metal-rich RR Lyrae have a long-period ($P \gtrsim 1000$ d) A, F, G or K-type companion. Observationally characterising the orbital periods and masses of such stellar companions will provide valuable new constraints on mass and angular momentum-loss efficiency for Sun-like accretors and the nature of RR Lyrae populations.

Key words: stars: variables: RR Lyrae – Galaxy: kinematics and dynamics – Galaxy: stellar content – Galaxy: halo – Galaxy: disc

1 INTRODUCTION

1.1 Classical RR Lyrae

RR Lyrae variables are one of the best-known types of stellar pulsators (Catelan 2004, 2009). These helium-burning horizontal branch (HB) stars are believed to come from an old (> 10 Gyr) metal-poor ([Fe/H] $\lessapprox -1$) stellar population. They are located in the instability strip (IS) in a compact region of the Hertzsprung-Russel (HR) diagram. Their chemistry, evolution and lightcurve properties are well understood, making these stars an excellent probe of stellar pulsations and stellar evolution (Smith 2004). Since RR Lyrae are easy to identify, one can use them to discover faint old metal-poor objects such as dwarf galaxies or globular clusters, e.g. Sesar et al. (2014); Torrealba et al. (2019).

Thanks to their relatively narrow colour range, RR Lyrae have been used to measure reddening and probe the interstellar medium (ISM), e.g. Haschke et al. (2011). Similarly, since their luminosity at a given metallicity is accurately known, RR Lyrae are one of the primary standard candles. The accuracy of RR Lyrae as standard candles has recently been improved thanks to the data from *Gaia* (Muraveva et al. 2018b; Holl et al. 2018). As standard candles, RR

★ bobrick@campus.technion.ac.il — equally contributing co-first author
† giuliano.iorio.astro@gmail.com — equally contributing co-first author

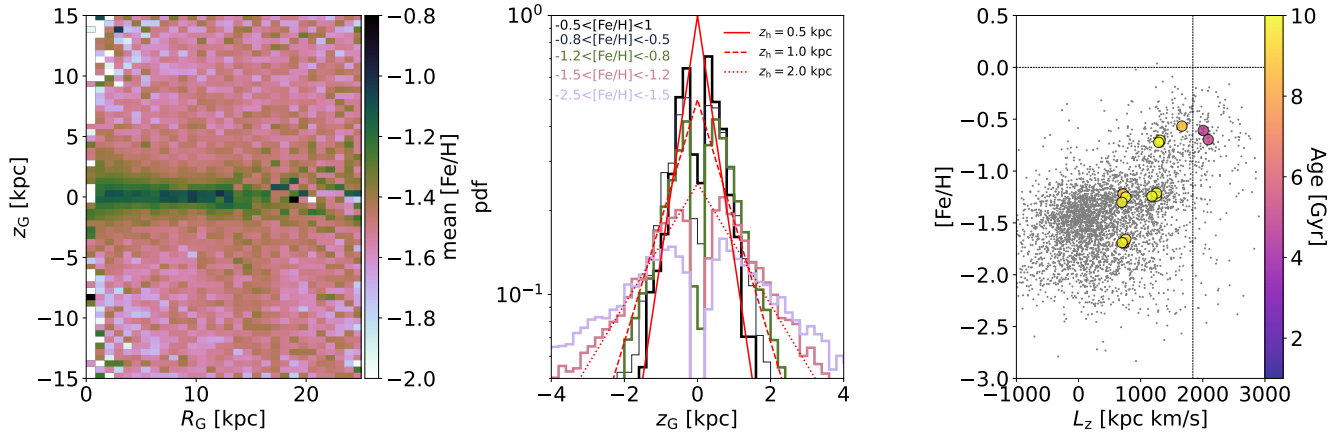

Figure 1. Properties of RR Lyrae stars in the *Gaia* DR3 catalogue (Clementini et al. 2022). *Left panel*: Mean metallicity in bins of R_G (Galactic cylindrical radius) and z_G (height above the Galactic plane). *Middle panel*: Vertical distribution of RR Lyrae in different metallicity bins. The red lines show exponential distributions with scale heights: 0.5 kpc, solid line; 1.0 kpc, dashed line; 2.0 kpc dotted line. The lack of sources at $z_G \approx 0$ is an observational bias due to an increase in the Galactic extinction. *Right panel*: Distribution of *Gaia* DR3 RR Lyrae (grey dots) in the vertical Galactic angular momentum ($L_z = R_G V_{\phi_G}$)-metallicity ([Fe/H]) plane. The coloured circles indicate the population's age derived from the vertical velocity dispersion using the Sharma et al. (2020) relations. Each circle indicates a given bin in L_z (bins edges: 500, 1000, 1500, 1800, 2500, 3000 kpc · km · s^{-1}), absolute Galactic height $|z_G|$ (bins edges: 0, 0.5, 1.0, 1.5 kpc) and metallicity (bins edges: −3.0, −2.0, −1.5, −1.0, 1.0), and only bins with more than 30 stars are shown. The positions of the circles indicate the median value of L_z and the metallicity of the stars in the bin. The velocity dispersions have been estimated by minimizing a Gaussian likelihood with centroid $\langle V_z \rangle = 0$ and considering the contribution of the velocity uncertainties. The dashed gray lines indicate [Fe/H] = 0 and $L_z = 1840$ kpc · km · s^{-1} (the latter value is obtained based on $R_G = 8$ kpc and $V_{\phi_G} = 230$ km · s^{-1}). In the first two panels, we use all the 130557 RR Lyrae classified as RRab or RRc with an available estimate of the period and other light curve parameters (e.g. ϕ_{31}) and with a reddening value (ebv) smaller than 2 (based on the Schlafly & Finkbeiner 2011 reddening map). In the third panel, we use a subsample of 4039 RR Lyrae satisfying the conditions described above and with available radial velocities in the GDR3 catalogue. The metallicities and the distance have been estimated as in Iorio & Belokurov (2021). The Sun is assumed to be located at $(x_G, y_G, z_G) = (8.13, 0, 0)$ kpc in the Galactic Cartesian coordinates (Gravity Collaboration et al. 2018; Iorio & Belokurov 2021), with cylindrical velocities $(V_{R_G}, V_{\phi_G}, V_{z_G}) = (-11.10, 250.24, 7.25)$ km · s^{-1} (Schönrich et al. 2010; Schönrich 2012; Iorio & Belokurov 2021).

Lyrae stars have been used to measure the distances to globular clusters and nearby galaxies with ∼2% accuracy, e.g. Sarajedini et al. (2006); Braga et al. (2015). They have also been used in constructing the cosmological distance ladder for nearby galaxies, complementing the distances from the brighter Cepheid variables (Beaton et al. 2016; Riess et al. 2016). Furthermore, since RR Lyrae belong to an old Galactic stellar population, they have been extensively used to characterise the substructures in the Galactic Halo and reconstruct the Milky Way merger history, e.g. Fiorentino et al. (2015); Belokurov et al. (2017); Fiorentino et al. (2017); Iorio et al. (2018); de Boer et al. (2018); Iorio & Belokurov (2019). Finally, RR Lyrae pulsators have provided a wealth of information on the structures and formation histories of the Galactic Thick Disc, Bulge, Magellanic Clouds, dwarf spheroidals and other galaxies in the local group, e.g. Feast et al. (2008); Pietrukowicz et al. (2015); Gran et al. (2015); Monelli et al. (2018); Muraveva et al. (2018a, 2020); Cusano et al. (2021); Iorio & Belokurov (2021).

The physics behind the RR Lyrae pulsations is well understood (Smith 2004). An HB star consists of a hot helium-burning core surrounded by a relatively thin and cold H envelope. The envelope reprocesses the radiation from the stellar core, thus shifting its spectrum redwards. Therefore, the mass of the envelope and its opacity dictate the effective temperature of the star and its position along the HB. The RR Lyrae variability, as well the variability of other stars in the IS, is produced by radial pulsation of the stellar layers driven by the so-called $\kappa - \gamma$ mechanism. In the stellar interior, the H and He layers are partially ionized and act as a "thermodynamic" valve trapping energy during compression and releasing it during expansion, allowing the full development of radial oscillations (Catelan & Smith 2015, and references therein).

Low-mass Sun-like stars ($M_{\rm init} \lesssim 2\,M_\odot$) go through the He core flash before landing on the HB. Therefore, on the HB, they have similar He-cores ($M_{\rm core} \approx 0.5\,M_\odot$) with similar luminosity nearly independent of the progenitor mass. Conversely, the temperature and colour of HB stars depend mainly on the amount of H-envelope and its opacity. The opacity, in turn, is sensitive to metallicity, with more metal-rich stars being more opaque, better at reprocessing radiation and hence redder. Therefore, metal-poor stars ([Fe/H] $\lesssim -1.0$) with initial masses of $0.7 - 0.8\,M_\odot$ have sufficiently low-mass envelopes and sufficiently low opacity so that they become hot enough to land in the IS. Since the typical main-sequence lifetimes of such stars are long, > 10 Gyr, these are old population-II stars. Such -ld metal-poor "classical" RR Lyrae represent the bulk of the RR Lyrae in the Stellar Halo and globular clusters.

1.2 Metal-Rich RR Lyrae

It is hard to produce metal-rich RR Lyrae within the classical scenario. The atmospheres of old metal-rich HB stars are more opaque to the radiation and appear redder than otherwise similar old, metal-poor stars. Therefore, they must have a less massive envelope to enter the IS. Since more metal-rich stars evolve slower[1] and need

[1] The stellar cores in metal-rich low-mass stars are larger and colder than in their metal-poor counterparts. Consequently, the efficiency of hydrogen burning is lower, and the metal-rich stars live longer. According to the MIST stellar tracks (Choi et al. 2016, see Section 2.2), a star with initial mass

a smaller initial mass to have thinner envelopes on the HB, there is an age-metallicity correlation among classical RR Lyrae, with higher-metallicity classical RR Lyrae being older (see, e.g. Savino et al. 2020). At least in principle, metal-rich stars can enter the IS either by starting with a lower initial mass ($M_{\rm init} \lesssim 0.7\,{\rm M}_\odot$) or via a significant mass loss on the Red Giant Branch (RGB). However, as we discuss in detail in Section 4, the absence of evolved stars less massive than $0.7\,{\rm M}_\odot$ and the observational constraints on the RGB mass loss prevent RR Lyrae formation at metallicities above $[{\rm Fe/H}] \gtrsim -0.5$.

On the other hand, the observations of the Galactic metal-rich RR Lyrae challenge the classical formation scenario. Despite the classical interpretation of RR Lyrae as old and metal-poor population II stars, metal-rich RR Lyrae stars are well-known to exist in the solar vicinity. These objects reach metallicities as high as $[{\rm Fe/H}] \approx 0.2$ and their vertical Galactic distribution, kinematics (Layden 1995a,b; Maintz & de Boer 2005; Marsakov et al. 2018; Liu et al. 2013; Prudil et al. 2020; Zinn et al. 2020; Gilligan et al. 2021), and chemical abundances are consistent with the Thin Disc (Marsakov et al. 2019; Crestani et al. 2021), although there are hints of an abundance deficiency for some elements such as Aluminium (Feuillet et al. 2022) and Scandium (Gozha et al. 2021).

Iorio & Belokurov (2021) exploited the unprecedented RR Lyrae catalogue from *Gaia* DR2, confirming that the population of metal-rich RR Lyrae is not limited to the Solar neighbourhood but permeates the Thin Disc from the inner parts (≈ 3 kpc) out to the disc's outskirts (≈ 25 kpc). Surprisingly, the kinematics of this population (circular velocity and velocity dispersions) is consistent with the young Thin Disc ($\lesssim 7$ Gyr, Ablimit et al. 2020; Sharma et al. 2020, see also Prudil et al. 2020). The existence of such a metal-rich and likely young population is a conundrum. Either they are indeed young, challenging the classical formation scenario of RR Lyrae stars, or they are one of the oldest Milky Way populations that somehow remained completely unperturbed during the turbulent past of our Galaxy (see, e.g. Belokurov et al. 2018; Myeong et al. 2019). The existence of such a population is also in tension with the recent discovery of an ancient pre-disk state of our Galaxy (see Belokurov & Kravtsov 2022; Conroy et al. 2022; Myeong et al. 2022).

The third *Gaia* data release (GDR3, Babusiaux et al. 2022) further supports the presence of a large population of RR Lyrae in the young Thin Disc. The new data release includes a dedicated catalogue of more than 270 000 RR Lyare (Clementini et al. 2022). About half of this sample contains a complete characterisation of the lightcurves (periods and Fourier transform parameters) that can be used to retrieve the photometric metallicity and a robust estimate of distance (see, e.g., Iorio & Belokurov 2021; Mullen et al. 2021; Li et al. 2022b). In Figure 1, we show an overview of the chemical, spatial and kinematic properties of this sample. The left-hand panel clearly shows the metallicity gradient as a function of the Galactic height, $z_{\rm G}$. At high $|z_{\rm G}| \gtrsim 5$ kpc, the sample is dominated by metal-poor RR Lyrae ($[{\rm Fe/H}]$ between about -1.7 and -1.5) that belong to the Stellar Halo. Around $|z_{\rm G}| = 3$ kpc, the mean metallicity starts to increase from $[{\rm Fe/H}] \approx -1.3$ to solar-like values, $[{\rm Fe/H}] \approx -0.5$, very close to the Galactic plane at $|z_{\rm G}| < 0.5$ kpc. Part of the population in this region is not visible due to the Galactic extinction and, therefore, it is larger than shown in the figure. The flattened metal-rich component extends all over the Galactic disc from the inner parts (at galactocentric radii $R_{\rm G} \approx 1$ kpc) to the very outer disc ($R_{\rm G} \approx 25$ kpc). It is important to notice that the Stellar Halo RR Lyrae are present also at low Galactic heights (see, e.g., Iorio & Belokurov 2021); therefore, the gradient of the mean metallicity is in part driven by the evolution of the halo-to-disc fraction (Iorio & Belokurov 2021).

As may be seen from the middle panel in Figure 1, the most metal-rich RR Lyrae have a relatively thin vertical distribution consistent with an exponential model with a vertical scale height of ≈ 0.5 kpc. This value is roughly consistent with the vertical scale height of the Galactic stellar Thin Disc of 0.3 – 0.5 kpc (e.g. Bovy et al. 2016). The population with metallicities between -1.2 and -0.8 follows an exponential profile with a vertical scale height of 0.9 – 1 kpc, consistent with the scale height of the Galactic Thick Disc (e.g. Jurić et al. 2008). At higher metallicities, the vertical profile rapidly broadens (scale height larger than 2 kpc), setting the transition into the spheroidal Stellar Halo component.

The metal-rich RR Lyrae population not only occupies a space-volume consistent with the Galactic Thin Disc but also shows cold kinematics (low velocity dispersion) typical of young stars in the Thin Disc. Since we expect that colder populations are also younger, the velocity dispersion can be used to estimate the population age (see, e.g., Sharma et al. 2020). The right-hand panel shows the result of applying the Sharma et al. (2020) model to a subsample of GDR3 RR Lyrae with full available phase-space information. There is a clear age transition from the old ($\gtrsim 8$ – 10 Gyr) Halo/Thick Disc population (low $L_{\rm z}$ and $[{\rm Fe/H}]$) to the younger Thin Disc population ($\lesssim 7$ Gyr). However, we warn the reader that the absolute ages reported in Figure 1 could be affected by the uncertainties that have not been considered in this simple analysis. Despite these uncertainties, one may see an age gradient reflecting the gradient in velocity dispersion as a function of the RR Lyrae metallicity.

In conclusion, this first examination of the RR Lyrae in GDR3 confirms the presence of a cold Thin Disc-like population composed mostly of metal-rich RR Lyrae. The kinematics of this population is consistent with a typical young population in the Galactic Thin Disc, and it is challenging to explain such RR Lyrae through the classical formation scenario in which RR Lyrae must be old and metal-poor.

1.3 Binary Metal-Rich RR Lyrae

Binary interactions can provide an alternative source of mass loss required to form young and metal-rich RR Lyrae. Such mass loss can be realised, for example, by material stripping by a binary companion through Roche-lobe overflow, e.g. Hurley et al. (2002), or tidal enhancement of wind mass loss, e.g. Tout & Eggleton (1988).

Systematic searches for RR Lyrae in binaries have produced more than 500 candidates using different methods: light time travel effect (e.g. Li & Qian 2014; Hajdu et al. 2015; Liška et al. 2016b,a; Li et al. 2018; Prudil et al. 2019; Hajdu et al. 2021), astrometric anomalies (e.g. Kervella et al. 2019a,b), radial velocities (e.g. Barnes et al. 2021), eclipses (e.g. Soszyński et al. 2009; Richmond 2011; Soszyński et al. 2011) or high-resolution images (e.g. Salinas et al. 2020). However, the large majority of the candidates still lack a definite confirmation, and some systems have been already rejected (see, e.g. Salinas et al. 2020).

Currently, there are only two robust confirmations of RR Lyrae in binary systems: the field star TU UMa (Szeidl et al. 1986; Saha & White 1990; Kiss et al. 1995; Wade et al. 1999; Liška et al. 2016b) and the eclipsing variable OGLE-BLG-RR Lyrae YR-02792 in the Bulge (Soszyński et al. 2009; Pietrzyński et al. 2012; Smolec et al.

$0.9\,{\rm M}_\odot$ leaves the main sequence approximately after 7 Gyr for $[{\rm Fe/H}] = -2$, after 13 Gyr for $[{\rm Fe/H}] = 0$, and after 16 Gyr for $[{\rm Fe/H}] = 0.3$.

2013). Although the Bulge star light curve closely resembles the one of classical RR Lyrae, it has been defined as an RR Lyrae "impostor" since its low mass ($0.26\,M_\odot$) and some other pulsation properties are not consistent with the classic RR Lyrae stars (Smolec et al. 2013). Given the peculiar low mass of this system, Pietrzyński et al. (2012) proposed that it is produced through mass transfer in the binary system and considered this star as the prototype of a new class of objects dubbed Binary Evolution Pulsators (BEP).

Motivated by the BEP discovery, Karczmarek et al. (2017) made use of the population synthesis STARTRACK code (Belczynski et al. 2008) to model the population of binaries among RR Lyrae and Cepheid pulsators at solar-like metallicity ($Z_\odot = 0.02$). They found that mass transfer allows stars to enter the IS through various routes that can be categorised into three main channels. In the dominant channel, the stripped donor star ignites helium and lands on the IS as an HB star[2]. In the less frequent cases, RGB or Asymptotic Giant Branch (AGB) stars cross the IS *while* being stripped by the companion, leading to short-lived objects. In the dominant HB channel in the Karczmarek et al. (2017) study, most of the produced RR Lyrae are young ($< 2\,$Gyr) and, therefore, originate from $\gtrsim 1.8\,M_\odot$ progenitors. The authors conclude that binary-produced RR Lyrae stars represent only a tiny fraction of the total RR Lyrae population ($< 1\%$). However, their estimated binary population of BEPs is not normalised by the total Galactic mass or the masses and metallicities of its components. In this paper, we model the dominant binary RR Lyrae formation channel proposed by Karczmarek et al. (2017) where the RR Lyrae stars form as previously stripped HB stars that land on the IS and argue that this channel can fully explain the Galactic population of metal-rich RR Lyrae.

1.4 Present Study

The dominant channel of binary RR Lyrae formation in the Karczmarek et al. (2017) study represents the stars stripped on the RGB by a binary companion so that after stripping, they retained an appropriately thick envelope to land in the IS. This channel is closely related to a larger population of all the stars stripped on the RGB by a binary companion and retaining envelopes of varying thicknesses. As we discuss in Section 2, such interactions on the RGB are common and happen in approximately 25 per cent of binary stars and 10 per cent of all the Galactic Sun-like single or binary stars. Among this larger population of stellar products resulting from binary stripping on the RGB, the population of long-period hot composite subdwarf B (sdB) type stars is, presently, characterised the best.

Similarly to the majority of binary RR Lyrae pulsators, hot composite sdB binaries are also core-helium burning stars stripped by a binary companion, e.g. Han et al. (2000, 2002); Chen et al. (2013). However, unlike binary RR Lyrae pulsators, sdB stars have been fully stripped of hydrogen. They are therefore bluer and much hotter than their RR Lyrae counterparts, thus lying outside the IS. Since binary sdB stars can be observed as spectroscopically double-lined binaries, their orbits can be well characterised (Heber 2016). Additionally, since these systems form through only one phase of mass transfer, they are believed to be excellent and constraining probes of mass transfer in binaries. Currently, there are 23 hot composite sdB binaries with known orbital periods and mass ratios (Vos et al. 2019).

Recently, Vos et al. (2020) performed Galactic population synthesis of hot composite sdB binaries with a detailed population synthesis code Modules for Experiments in Stellar Astrophysics (MESA, Paxton et al. 2011, 2013, 2015, 2018, 2019). By modelling a population of binaries calibrated by the Galactic metallicity and star formation history, Vos et al. (2020) have been able to *simultaneously* reproduce the observed periods, mass ratios, metallicities and formation rates of hot composite sdB binaries without explicitly fitting any parameters.

Since the Vos et al. (2020) modelled all the Galactic binaries that were stripped on the RGB, their population also includes the binary RR Lyrae progenitors. Compared to Karczmarek et al. (2017), Vos et al. (2020) used a standard model of binary mass transfer and a standard model of Galactic evolution. Furthermore, the majority of the present-day long-period sdB and HB stars come from solar-like ($M_{\rm primary} \lesssim 2\,M_\odot$) binaries that ignite their helium core degenerately through a helium flash. Since the current population synthesis codes do not have correct helium ignition conditions, one must use detailed stellar structure codes like MESA to correctly evolve stars through the helium core flash and match the observed properties of sdB binaries (Vos et al. 2020). Altogether, given the very good agreement of the modelled population with the observed hot composite sdB binaries, where the RG progenitor is fully stripped, we also expect a good agreement with the observed properties of the binary RR Lyrae, where the RG progenitor is stripped partly. Importantly, since binary stripping affects stars of all metallicities, metal-rich stars can land in the instability strip as RR Lyrae pulsators.

In this study, following Karczmarek et al. (2017) and Vos et al. (2020), we use a detailed stellar structure code MESA to investigate the Galactic population of binary RR Lyrae that were previously stripped by a binary companion on the RGB. We show, in particular, that the RR Lyrae produced through this channel are common and likely make all of the metal-rich Galactic RR Lyrae globally and even dominate the RR Lyrae population in the Solar Neighbourhood. We summarise the population setup and the RR Lyrae formation scenario in Section 2. We further present the observational properties of the binary RR Lyrae population in Section 3, arguing that they provide a natural explanation for the Galactic population of metal-rich RR Lyrae that is consistent with the current observations. Finally, we discuss the implications of our modelling in Section 4.

2 BINARY AND SINGLE EVOLUTION MODELLING

2.1 Formation Scenario

We summarise the two dominant formation channels for RR Lyrae in Figure 2. In the Binary Channel, the progenitor is a close binary ($100\,{\rm d} \lesssim P_{\rm orb} \lesssim 700\,{\rm d}$) that consists of two Sun-like main sequence stars in the field, such that the more massive primary ignites helium degenerately through a helium flash ($0.7\,M_\odot \lesssim M_{\rm primary} \lesssim 2\,M_\odot$). As the primary star evolves, it becomes a red giant and overflows its Roche lobe, non-conservatively transferring mass to the companion. If the red giant is sufficiently evolved by the time of Roche lobe overflow and has a sufficiently massive core, it ignites its core through a helium flash. Helium ignition typically happens while mass transfer is ongoing. The stripped red giant remnant thus becomes an HB star similar to the HB stars produced from a Single Channel, albeit with a partly stripped envelope.

[2] The fact that the HB channel dominates the RR Lyrae population in the Karczmarek et al. (2017) may not be evident directly from the study. However, this may be readily appreciated from the bottom panel in Figure 5 of the paper, together with the fact that the panel shows a log-linear plot.

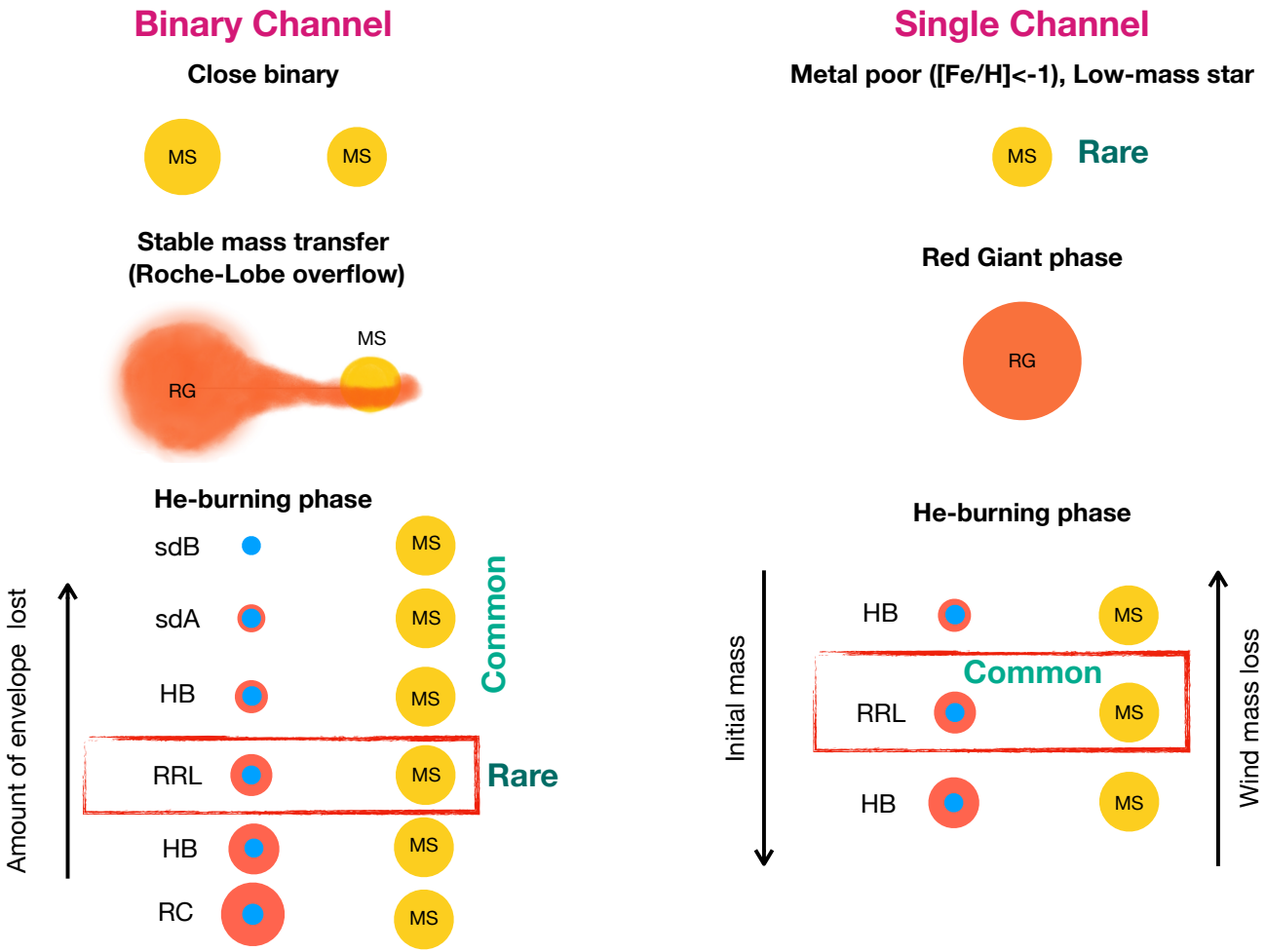

Figure 2. Two main formation channels for RR Lyrae stars. In the Binary Channel, a typical main-sequence star (MS) gets stripped by a companion and ignites helium (a common process). The red giant (RG) may be stripped of nearly all its hydrogen envelope, producing a hot subdwarf A or B (sdA or sdB) star. If the red giant is stripped of only a fraction of its envelope, it produces a horizontal branch star (HB, common process). A fraction of such HB stars will fall in the instability strip producing RR Lyrae stars (RR Lyrae, a rare outcome). In the Single Channel, typical metal-rich stars ($[\mathrm{Fe/H}] \gtrsim -1$) have too thick envelopes on the HB to enter the instability strip and instead become the so-called red-clump stars (RC). However, when a metal-poor old low-mass star ($[\mathrm{Fe/H}] < -1$, rare object) evolves into an HB star, it typically has a sufficiently thin and transparent envelope to commonly end up in the instability strip through regular single stellar evolution. Such HB stars are observed as RR Lyrae. Without an envelope stripping phase, the final amount of the envelope in the HB depends solely on the initial mass of the star and the wind mass loss through the Red Giant phase. Although both channels have comparable production rates in the Milky Way, the old metal-poor RR Lyrae produced through the Single Channel have been studied extensively since they commonly occur in the metal-poor Halo of our Galaxy while their younger metal-rich binary counterparts have been hiding in the Galactic disc.

The exact dynamics of mass transfer is governed by the interplay of stellar evolution, the response of the donor to mass loss, the feedback of mass transfer on the orbital separation and the resulting effect on the degree by which the donor overflows its Roche lobe, and hence the mass transfer rate, e.g. Tauris & van den Heuvel (2006); Bobrick et al. (2017); Vos et al. (2020). In particular, the donor red giant tends to expand upon mass loss and contract after igniting helium. While we employ a detailed binary stellar evolution code to model the interplay of these processes, as we describe in Section 2.2, we mention at this point that the resulting HB star can experience a wide range of the degrees of stripping and thus have a range of envelope masses.

The larger fraction of the envelope gets stripped, the more the He core of the HB star is exposed, and the bluer it becomes. In the limit of negligible stripping, the remnant is indistinguishable from an HB star from a Single Channel. Conversely, in the limit of complete stripping, the naked helium-burning core remnant is observed as a hot sdB star. In the case of partial stripping, the surface temperatures may place the remnant in the instability strip. Since the HB star, apart from surface stripping, is otherwise similar to single HB stars, it will produce pulsations closely resembling those of classical RR Lyrae. Since the Binary Channel can operate at any metallicity, binary stripping allows metal-rich HB stars to acquire the thin envelopes they need to become RR Lyrae.

In the Single Channel, the progenitors are metal-poor ($[\mathrm{Fe/H}] \lesssim -1$) old stars, such as the stars frequently encountered in the Galactic Thick Disc or Halo. Such progenitors produce HB stars as a natural outcome of their single stellar evolution. The typical single HB stars in the Galaxy are too red to be in the IS. However, metal-poor stars have less opaque and hence bluer envelopes. In

addition, they evolve faster than the field population and can have a smaller initial mass compared to more metal-rich stars. Since the helium core mass in HB stars is always close to about $0.4 - 0.5\,M_\odot$, such old, metal-poor stars have the lowest-mass envelopes. The combination of these effects places such single stars on the IS.

In the Binary Channel, a population of field binaries experiences a common process of binary mass transfer, which may produce RR Lyrae in the relatively rare case when the stripping places the remnant in the IS. In comparison, in the Single Channel, a relatively rare old and metal-poor population follows a common process of single stellar evolution, this way also producing RR Lyrae pulsators. Subsequently, we show that these two processes, with Common×Rare and Rare×Common probabilities, correspondingly, produce present-day RR Lyrae at comparable rates. Since the Single and Binary Channels operate, correspondingly, at low and all metallicities, the combined action of both channels, therefore, can simultaneously explain the populations of metal-poor and metal-rich RR Lyrae.

2.2 Single and Binary Modelling

We set up the Galactic population of all the present-day HB stars closely following the setup used in Vos et al. (2020) and summarise only the most important aspects here.

We initialise the Galactic population using the Besançon model (Robin et al. 2003), a standard Galaxy model calibrated by large-scale photometric surveys. Within the model, the Galactic population of stars is split into 10 bins: 7 bins for the Thin Disc and 1 bin for the Thick Disc, Halo and the Bulge, each with its mass and metallicity distribution. We normalise the total present-day stellar mass of the Galaxy to $M_{\rm MW} = 6.43 \cdot 10^{10}\,M_\odot$ following McMillan (2011). We obtain the mass fractions of the Thin Disc by integrating the density profiles from Robin et al. (2003) and use the recent measurements for present-day stellar masses of the Thick Disc and Bulge from Robin et al. (2012, 2014) and Halo from Deason et al. (2019). This way, by randomly assigning each simulated object a Galactic bin, formation time and metallicity, following the Besançon model, we can keep track of the Galactic mass represented by each simulated object.

As the next step, we initialise a collection of binaries and single stars for the detailed stellar evolution modelling. The masses of single stars and the primary stars in binaries are drawn from the Kroupa & Haywood v6 initial mass function (IMF) model from Czekaj et al. (2014), as used in the Besançon model (see also Kroupa 2008; Haywood et al. 1997). Since we are interested in present-day RR Lyrae and since all helium-burning stars exist for up to about 100 Myr, we only select the primaries that reach the tip of the RGB not earlier than 300 Myr ago and not more than 700 Myr in the future. Furthermore, we are only interested in binaries that may become core-helium burning stars. Therefore, we consider binaries with initial periods between 100 d and 700 d, i.e. binaries in which the primary stars have developed a sufficiently massive core needed for helium ignition by the time of mass transfer. Finally, we focus only on the binaries with the primary mass between $0.7\,M_\odot$ and $2.1\,M_\odot$ that ignite their cores degenerately. Such binaries lead to RR Lyrae that have core masses similar to the RR Lyrae from the classical Single Channel, and the models of preceding mass transfer in such binaries are in detailed agreement with the present-day long-period hot composite sdB populations. In contrast, the core masses of the HB stars that enter the IS after non-degenerate ignition are typically different from the canonical mass, and their orbital and companion properties may be affected by choice of the mass transfer model parameters. Therefore, in the scope of this study, we focus only on degenerately-igniting systems.

We draw the binary companion masses from a uniform distribution in q^{-1} (Raghavan et al. 2010), where $q \equiv M_{\rm primary}/M_{\rm secondary}$ in the range between 0 and 3, which fully encloses the binaries for which mass transfer proceeds stably. In comparison, all the binaries with $q > 3$ experience a common envelope phase. In this case, the binary companion and the core of the giant spiral into a short-period orbit ($P_{\rm post-CE} \lesssim 5$ d). For such post-common envelope systems, the core gets stripped so much that no HB star (and hence no RR Lyrae) can be produced, consistently with the lack of observed HB stars with short-period companions, e.g. Vos et al. 2022 (in prep). We draw the binary orbital periods from the suitable log-uniform distribution from Abt (1983) for close binaries with periods between 1 and 10^4 d. We then select the binaries in the mentioned 100 – 700 d period range for detailed simulation. We assumed circular orbits for all the simulated binaries since red giants typically circularise by tides by the time they overflow the Roche lobe (Vos et al. 2015). Finally, to associate each single or binary star with the stellar mass it represents in the Galaxy, we used the total binary fraction of 0.45 and the close binary fraction (the fraction of binaries that have their period in the range of $1 - 10^4$ d) equal to 0.25 (Moe et al. 2019, see also Li et al. 2022a).

We model the Galactic binary population of RR Lyrae by simulating 2060 potential RR Lyrae progenitors in the detailed binary evolution code MESA, version r10390. We employ a standard model of mass loss by the binaries, in which binaries are conservative until the accreting star reaches super-critical rotation (Popham & Narayan 1991; Paczynski 1991; Deschamps et al. 2013), which happens typically at mass transfer rates of $10^{-5} - 10^{-6}\,M_\odot$/yr. Once the accretor reaches super-critical rotation, mass transfer is assumed to proceed fully non-conservatively with the carried away specific angular momentum equal to that of the accretor. Apart from being established theoretically, e.g. Soberman et al. (1997); Paxton et al. (2015), the non-conservativeness for such progenitor systems is strongly supported by the observations of long-period hot composite sdB binaries (Vos et al. 2020). At the same time, the theoretically expected angular momentum loss model is yet to be entirely constrained by observations. We discuss the possible effects of other angular momentum prescriptions in Section 4. Finally, we use the Neural Network-Assisted Population Synthesis code NNAPS[3] to extract the stellar parameters from the MESA runs.

To compare the binary RR Lyrae population to the classical Single Channel or RR Lyrae in the same Galactic model, we simulate a Galactic sample of 10000 single progenitors of present-day HB stars interpolating MIST tracks (Choi et al. 2016) using the population synthesis code SEVN (Iorio et al., in prep; Mapelli et al. 2020; Spera et al. 2019; Spera & Mapelli 2017). The MIST stellar tracks have been computed using the detailed binary stellar evolution code MESA (Dotter 2016), and therefore the comparison between the Single and Binary Channel is self-consistent regarding the stellar evolution model. We discuss alternative single evolution models in Section 4.3.1.

Since Halo and Thick Disc stars are also frequently found in binaries, the binary companion of a Halo star must be sufficiently far away for it to produce an RR Lyrae and be 'effectively single'. To account for this, we assume that solar-like Halo stars have the same binary fraction of 0.45 as the field stars and have a close binary fraction of 0.4, suitable for low metallicities [Fe/H] $\lesssim -1$

[3] NNaPS is available on GitHub

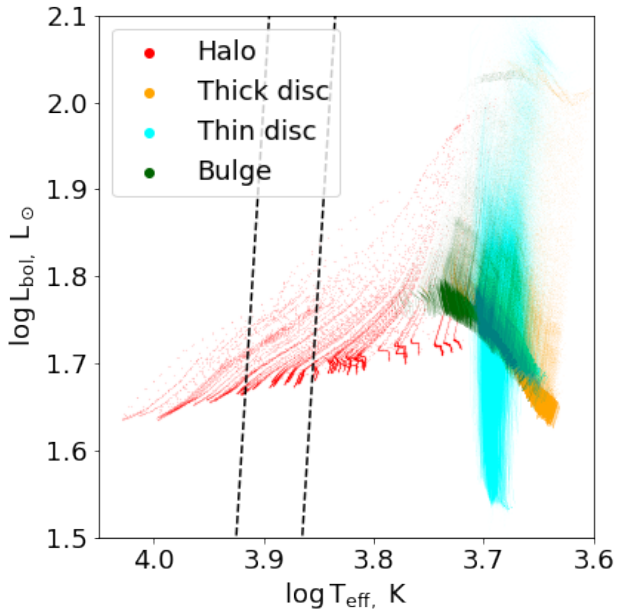

Figure 3. Evolution tracks for the single stars sampled from the Galactic model and evolved interpolating MIST stellar tracks in the population synthesis code SEVN (Iorio et al., in prep; Mapelli et al. 2020; Spera et al. 2019; Spera & Mapelli 2017, Section 2.2). Each point represents the properties of a given star at a certain time during the core-helium burning phase. Different colours indicate stars belonging to different Galactic components (Section 2.2): Stellar Halo (red), Thick Disc (orange), Thin Disc (cyan), Bulge (dark green). The black-dashed lines show red and blue limits of the instability strip (Equation 1).

(Moe et al. 2019). A star is treated as 'effectively single' if it does not overflow its Roche lobe when its radius reaches $1.2\,R_{\rm RG,max}$. In such a case, it will transfer mass to the companion neither on the RGB nor during the temporary expansion after the helium flash, e.g. Fainer et al. (2022). If a Halo star does get stripped by a binary companion, it will rarely land in the IS, as, e.g. may be seen in Figure 2. Therefore, we assume that metal-poor stars stripped by a binary companion cannot produce RR Lyrae.

For the purpose of this work, we define the instability strip boundaries following Karczmarek et al. (2017):

$$\begin{aligned} \log\left(\frac{T_{\rm red}}{\rm K}\right) &= -0.05\log\left(\frac{L}{\rm L_\odot}\right) + 3.94 \\ \log\left(\frac{T_{\rm blue}}{\rm K}\right) &= -0.05\log\left(\frac{L}{\rm L_\odot}\right) + 4.00 \end{aligned} \quad (1)$$

In the subsequent analysis, whenever appropriate, we consider the binary metal-rich populations of RR Lyrae in the field alongside the metal-poor Halo and Thick Disc RR Lyrae populations.

3 RESULTS

3.1 Single Stellar Evolution

In Figure 3, we show the MIST evolution tracks of stars during the core-helium-burning phase. The initial mass and metallicity of these stars are sampled from the same Galactic model as the one used in the binary analysis (Section 2.2). Only old (Age ≈ 14 Gyr), low-mass ($M_{\rm star} \approx 0.73\,{\rm M_\odot}$) and metal-poor ([Fe/H] $\lesssim -1.5$) stars in the Stellar Halo reach temperatures high enough ($T_{\rm eff} \gtrsim 7000$ K, $\log T_{\rm eff}/{\rm K} \gtrsim 3.85$) to enter in the instability strip. Stars belonging to the other Galactic components spend the core-helium burning phase in the red part of the HR diagram ($T_{\rm eff} \approx 5000$ K, $\log T_{\rm eff}/{\rm K} \approx 3.7$), forming the so-called red clump (RC). The Stellar Halo component is an efficient factory of RR Lyrae stars; about half (53 %) of stars belonging to the Halo component cross the IS during their core-helium-burning phase.

The combination of the Galactic model with the MIST stellar tracks at face value implies that no RR Lyrae stars can be produced in any Galactic components other than Halo through single stellar evolution. This scenario is likely an oversimplification due to the uncertainties in the stellar evolution (e.g. stellar winds and chemical compositions, see Section 4.3.1) and Galactic properties. For example, in the Galactic population model we use (Vos et al. 2020), the stellar ages in the Bulge range between 8 and 10 Gyr and the metallicity is larger than -1.2 at the 3σ level[4]. In contrast, Savino et al. (2020) found that the Milky Way Bulge hosts metal-poor ([Fe/H] $\lesssim -1.6$) and old RR Lyrae (Age $\gtrsim 13$ Gyr). The likely progenitors of these objects are not included in our Bulge sample. However, it is still unclear whether these RR Lyrae in the Bulge trace a clear separate Bulge component or just the inward extension of the stellar Halo (see, e.g. Navarro et al. 2021; Savino et al. 2020; Pérez-Villegas et al. 2017; Minniti et al. 1999). Moreover, even considering significant modifications in stellar evolution models (e.g. see Section 4.3.1, where we consider enhanced mass loss on the RGB), it is difficult to reach the RR Lyrae formation efficiency consistent with the observations of RR Lyrae in other Galactic components, especially considering the youngest populations (Age $\lesssim 8$ Gyr).

In conclusion, a clear bimodality emerges: in the Stellar Halo, the RR Lyrae stars are efficiently produced as a natural consequence of single stellar evolution. However, in the other Galactic components, the RR Lyrae production through single stellar evolution is inefficient or even absent. In such cases, it has to rely on enhanced mass loss or peculiar chemical compositions (see Section 4.3.1) and, generally, no plausible single stellar evolution models are capable of producing young RR Lyrae stars (Age < 7 Gyr). It is also worth mentioning that the in-situ part of the Stellar Halo (Belokurov et al. 2020; Belokurov & Kravtsov 2022) is more metal-rich than the rest of the Stellar Halo (see e.g. Iorio & Belokurov 2021). Hence, the alternative formation channels could have played a role in forming part of the RR Lyrae also in the in-situ Halo.

3.2 Physical Properties of Binary RR Lyrae

Binary RR Lyrae stars are a natural part of the population of binary stripped core-helium burning stars. As shown in Figure 4, they occupy a well-defined place in the continuum of all stripped core-helium burning stars on the $L - T_{\rm eff}$ diagram. Specifically, on the hotter end, at temperatures above 20000 K, binary core helium-burning stars are observed as blue hot composite sdB stars, neighbouring with yellower binary sdA stars with temperatures above 15000 K. On the colder end, a population of redder core-helium burning stars is observed as regular HB stars. These stars have a continuous range of temperatures between 4000 K and 15000 K, with 22 out of 507 (4.3 %) HB stars in our sample located in the IS.

The RR Lyrae in Figure 4 in our sample occupy a range of

[4] The age of the stars in the Bulge are drawn from a uniform distribution between 8 and 10 Gyr, while the metallicity distribution is a Gaussian with centre and standard deviation set at [Fe/H] = 0 and 0.4 dex, respectively

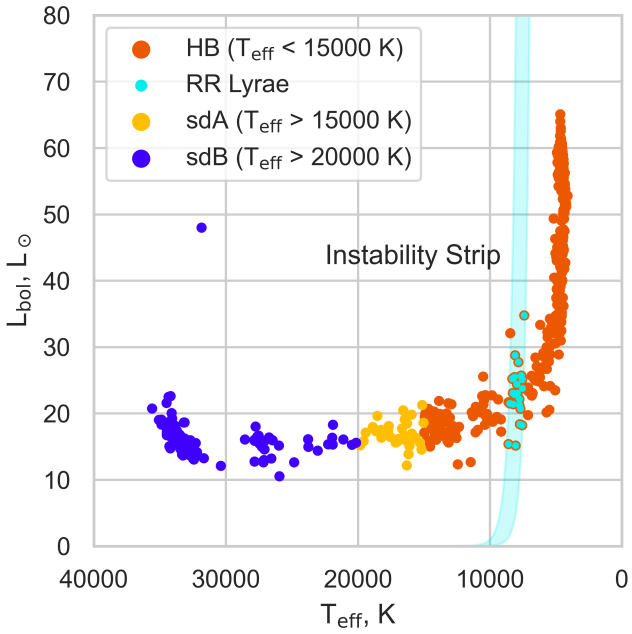

Figure 4. RR Lyrae are natural members of the population of core-helium-burning binary stripped stars. The HR diagram (bolometric luminosity versus the effective temperature) shows the stars stripped by their binary companions on the red giant branch (RGB) and igniting helium degenerately, based on our MESA models. Depending on the initial parameters, such as orbital periods and mass ratios, binary companions strip different fractions of the donor envelopes. Complete stripping leads to hot naked helium-burning cores observed as subdwarf B stars (sdBs). Near-complete stripping leads to colder subdwarf A stars (sdAs), whose envelope reprocesses the core radiation, making it cooler and redder. Partial stripping produces a continuum of red and cool stars observable as horizontal branch stars (HBs). A fraction of these HB stars lie on the instability strip and is observed as pulsating RR Lyrae stars.

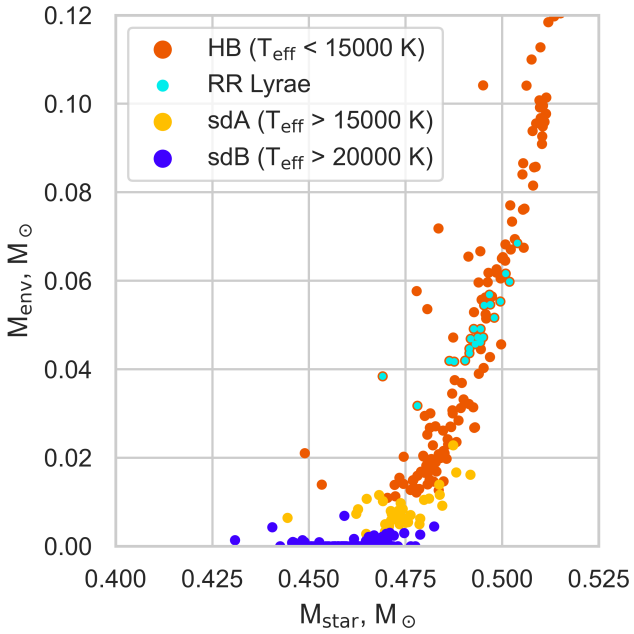

Figure 5. Structural properties of binary RR Lyrae. The figure shows the hydrogen envelope mass versus the total stellar mass for all the core helium-burning stars in our simulations. Hot subdwarf B (sdB) and subdwarf A (sdA) stars have thin, up to 0.02 $M_\odot$ envelopes. Photometrically redder horizontal branch (HB) stars can retain significant envelopes extending in mass beyond the range of the figure. The RR Lyrae stars stripped in binaries have between 0.03 and 0.07 $M_\odot$ envelopes and total masses between 0.47 and 0.50 $M_\odot$.

luminosities between 15 and 35 $L_\odot$, which is similar, although systematically fainter than the classical RR Lyrae from the Single Channel, which have luminosities closer to 45 – 50 $L_\odot$ (e.g., see Figure 3). Given that the cores of RR Lyrae from the Single and Binary Channels are nearly identical, the fact that the metal-poor RR Lyrae are brighter than the metal-rich RR Lyrae from the Binary Channel can be seen as a natural consequence of their metallicity. Indeed, metal-poor stars have lower opacity, making it easier for the inner nuclear burning regions to propagate the radiative energy to the stellar surface. Therefore, metal-poor stars are generally shorter-lived and more luminous than otherwise similar metal-rich stars (Bazan & Mathews 1990; Kippenhahn et al. 2013).

Structurally, the properties of binary RR Lyrae resemble those from the classical Single Channel. In Figure 5, we show the distribution of the envelope masses versus the total stellar mass for the sample of all the core-helium burning stars that ignited helium degenerately. The surface temperature of the stars correlates with the amount of hydrogen envelope left on the star, with the hottest sdB stars being nearly fully stripped of hydrogen ($M_{\rm sdB,env} \lesssim 0.007\,M_\odot$) and the HB stars having a range of envelope masses from about 0.01 $M_\odot$ and up to about 1.0 $M_\odot$. Since the majority of RR Lyrae have a narrow range of surface temperatures, they also have a relatively narrow range of envelope masses between 0.03 $M_\odot$ and 0.07 $M_\odot$. Furthermore, since the degenerate helium ignition occurs at roughly the same conditions, independently of the progenitor mass, the binary RR Lyrae have a narrow range of stellar masses between 0.47 $M_\odot$ and 0.50 $M_\odot$. Finally, since binary RR Lyrae have the same surface temperatures and core masses as the classical RR Lyrae, we expect their pulsation properties to be similar.

In contrast to the classical RR Lyrae from the Single Channel, binary RR Lyrae have a broad range of ages and metallicities. As we show in Figure 6, binary RR Lyrae form at all the Galactic epochs and metallicities. Therefore, most binary RR Lyrae trace the Galactic Thin Disc and tend to be young and metal-rich, with solar-like metallicities, and ages between 1 and 10 Gyr. Conversely, metal-rich and young environments or dynamically cold orbits may be a good indicator for binary RR Lyrae. Similarly to RR Lyrae from the Single Channel, it follows from our simulations that binary RR Lyrae show an anti-correlation between their luminosity and metallicity, and the envelope mass and metallicity.

As we show in Figure 7, binary RR Lyrae originate from binaries with primary masses in the range between 0.95 and 2.0 $M_\odot$ with mild mass ratios $q \equiv M_{\rm primary}/M_{\rm secondary}$ between 1.0 and 1.55. The initial periods of the progenitors are between 100 and 700 d, and the periods anti-correlate with the primary mass. The anti-correlation occurs because more massive stars evolve into smaller RGs and have shorter orbital periods at a given separation. We also have checked that all the systems we simulated fully enclose the parameter space of the RR Lyrae progenitors.

All RR Lyrae produced through the Binary Formation Channel have a binary companion. As we show in Figure 8, the present-day binary RR Lyrae have periods between 1000 and 1800 d, and companion masses between 0.65 and 1.9 $M_\odot$. In other words, the binary orbital periods increased due to mass transfer compared to

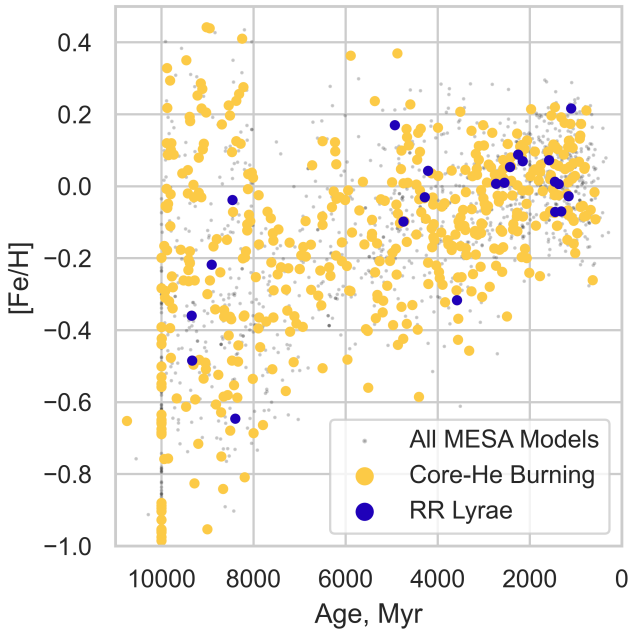

Figure 6. Age-metallicity plot for binary RR Lyrae in our synthetic population. On the horizontal axis, the age shows how long ago the RR Lyrae progenitors formed (recently formed systems are on the right). The vertical axis shows the initial metallicity of the progenitors. Generally, the distribution of RR Lyrae on the diagram resembles that of all core helium-burning stars and all the binaries in the Galactic population. However, there is a preference towards young ages and lower metallicities among binary RR Lyrae progenitors.

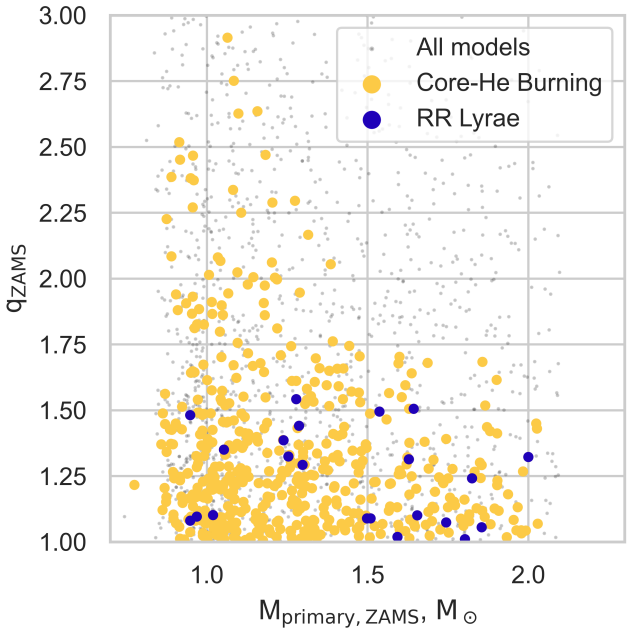

Figure 7. Progenitor properties for the metal-rich RR Lyrae population. The horizontal axis shows the initial masses of the primaries in our binary dataset. The vertical axis shows the binary mass ratios $q_{\rm ZAMS} \equiv M_{\rm primary}/M_{\rm secondary}$. The RR Lyrae progenitors are marked with dark blue points, the core-helium burning star progenitors are marked with yellow, and the systems that did not ignite helium are marked with grey. It may be seen that RR Lyrae progenitors occupy the full range of initial masses and prefer mild initial mass ratios $q_{\rm ZAMS} \lesssim 1.55$.

their initial values. The range of companion masses may be easy to explain by recalling that RR Lyrae progenitors had primary masses between 0.95 and 2.0 $M_\odot$ and mild mass ratios between 1.0 and 1.55. Furthermore, the initial primary mass correlates with age because present-day RR Lyrae recently ascended the RGB. Moreover, since, initially, the progenitor binaries had mild mass ratios, the present-day companion masses also correlate with age. In particular, only the systems younger than 3 Gyr have companion masses larger than 1 $M_\odot$ and, conversely, all the systems older than 3 Gyr have companion masses lower than 1 $M_\odot$. A similar correlation is present between the companion mass and the present-day metallicity, with all the systems bearing a $M_{\rm comp} \gtrsim 1\,M_\odot$ companion having a solar-like metallicity above [Fe/H] $\gtrsim -0.1$.

Many RR Lyrae from the Single Channel also have binary companions. In this case, however, the companion was on a sufficiently wide orbit, such that it did not perturb the single stellar evolution of the RR Lyrae progenitor. An example of such a system could be an old metal-poor star (e.g. 0.8 $M_\odot$, [Fe/H] = −1.5) that had a far away companion at 10^3 AU. In contrast to the Binary Channel, as we show in Figure 8, the orbital periods of such companions span a much wider range of more than 13 dex. In other words, the range of orbital periods that leads to stripping on the RGB is much narrower than the range of orbital periods needed for the secondary to not perturb the primary. However, since the red giants from the Single Channel only expand to about 80 – 100 $R_\odot$ due to their low metallicities (Choi et al. 2016) and since binary interactions did not widen their orbits as in the Binary Channel, the orbital periods of such binaries can be as small as 500 d. The companion mass range of RR Lyrae from the Effectively Single Channel also differs from the Binary Channel. Since the Single Channel represents an old population, the MS companions more massive than the RR Lyrae progenitors have already turned into white dwarfs, while the MS companions less massive than the RR Lyrae progenitors have present-day masses below about 0.75 $M_\odot$. Finally, a fraction of binary RR Lyrae from both Single or Binary Channels will have a wide-period tertiary or higher-order companion, e.g. Toonen et al. (2016).

3.3 Expected Observed Properties of Binary RR Lyrae

In Figure 9, we show a photometric HR diagram for stripped core-helium-burning stars, showing the *Gaia* eDR3 G-band magnitude and BP-RP colours. Most RR Lyrae from the Binary Channel occupy a relatively narrow range of colours between 0.1 and 0.4 and G-band magnitudes between 1.4 and 0.8. This range of magnitudes and colours is consistent with the observed metal-rich RR Lyrae, and the metal-rich end of the general (period-)luminosity-metallicity relation for all the observed RR Lyrae (Muraveva et al. 2018b; Li et al. 2022b). These predicted ranges of colours and magnitudes can be used to select candidate systems for follow-up observations.

While metallicity is the primary differentiating property between the Single and Binary Channels of RR Lyrae, direct detection of the binary companions will provide important confirmation for either scenario. Moreover, as we discuss in Section 4, measuring the properties of these companions may offer valuable new constraints for the binary evolution models.

As may be seen from Figure 9, an 11 per cent fraction of RR Lyrae from the Binary Channel (2 out of 22 systems in the Figure)

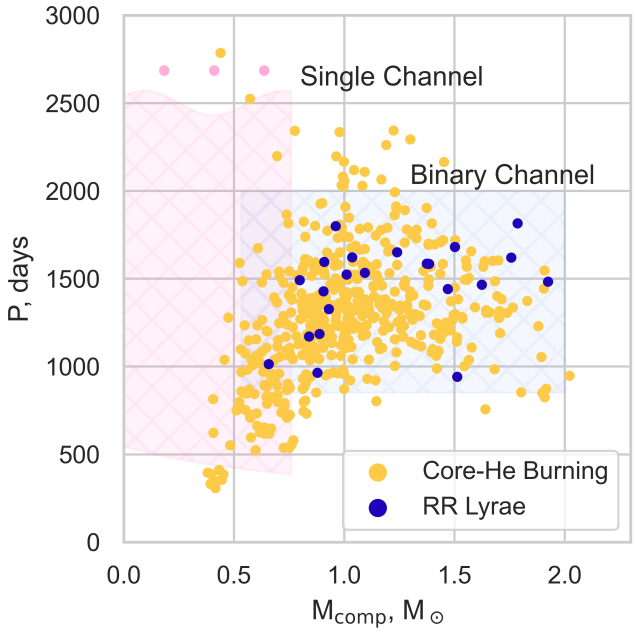

Figure 8. The companion properties (orbital period versus companion mass) of binary RR Lyrae. In the plot, the RR Lyrae from the Binary Formation Channel that ignited helium degenerately are shown in blue, and all the core-helium burning stars from the same channel are shown in yellow. The pink and blue shaded regions show the areas occupied by the binary RR Lyrae populations from the Effectively Single Channel and the Binary Channel, respectively. The companions of RR Lyrae from the Binary Channel have a relatively narrow range of orbital periods between 2.7 and 4.9 years and masses between 0.65 and 1.9 $M_\odot$. In contrast, while the RR Lyrae from the Single Channel may have a wide-period orbital companion that did not affect their earlier evolution, the distribution of such companions on this plot is much more sparse since their orbital period range is approximately 13 dex wider compared to the Binary Channel (the extended period range is shown with a break in the pink-shaded area). In particular, we estimate that about 1 in 60 Halo-like metal-poor RR Lyrae will have a companion with a period between 500 and 2000 d, while most of the companions will be on much wider orbits.

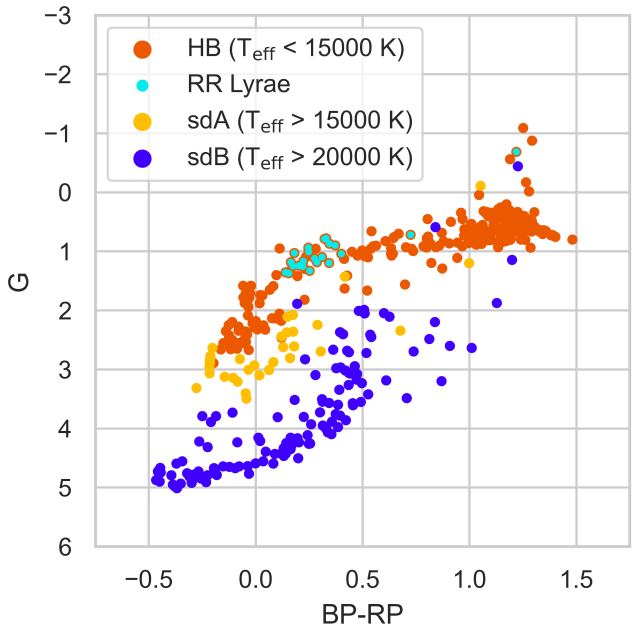

Figure 9. HR diagram in the *Gaia* eDR3 bands showing the photometric G-band magnitudes and BP-RP colours for the binary core helium-burning stars in our synthetic sample. Binary RR Lyrae from the Binary Channel occupy a compact region between the red weakly stripped horizontal branch (HB) stars on the right and photometrically bluer significantly stripped HB stars on the left. Due to their dominantly blue spectra and smaller radii, subdwarf A (sdA) and B (sdB) stars are typically dimmer in the G-band than binary RR Lyrae. The two RR Lyrae located away from the main clump of RR Lyrae contain a subgiant and giant companions. Such systems represent an example of objects exhibiting RR Lyrae pulsations outside of the instability strip (IS).

is located redwards from the main clump of RR Lyrae. These systems have an evolved companion that modifies the overall colour and G-band magnitude of the binaries, moving them closer to the RGB. Such systems are observationally interesting since they exhibit RR Lyrae pulsations away from the IS. In the Binary Channel, RR Lyrae may have evolved companions because even binaries with initial mass ratios close to unity may produce RR Lyrae. Similarly, in the Single Channel, approximately 0.3 per cent of all systems will have wide-orbit binary companions on the RGB. Such systems were born with near equal mass companions so that the secondary reaches the RGB shortly after the primary, i.e. while the primary is still an RR Lyrae. Located away from the IS, RR Lyrae with evolved companions likely have not been included in the spectroscopic or photometric selection functions. On the other hand, detecting and characterising such systems will put tight constraints on their progenitors and thus will be extremely valuable. Finally, we predict that approximately 0.03 per cent of metal-poor RR Lyrae have a wide-period binary companion which is also RR Lyrae. Such systems can only form in the Single Channel.

In Figure 10, we show the orbital properties for the binary RR Lyrae from the Single and Binary Channels. The properties of binary companions from both channels are notably different. The RR Lyrae in the metal-rich Binary Channel can have bright, close-by A, F, G and K-type companions. Indeed, such RR Lyrae have descended from relatively young binary progenitors and had companions with mild initial mass ratios. By now, all these RR Lyrae have been stripped to masses of $M_{\rm RRL} \approx 0.5\,M_\odot$ while their companion masses have changed little. Therefore, such systems always have more massive, comparably bright present-day companions with orbital velocities of $v_{\rm orb,comp} \lesssim 5\,$km/s. Due to smaller masses, the orbital velocities of RR Lyrae in this channel are larger, of order $v_{\rm orb,RRL} \gtrsim 7.5\,$km/s. In the Single Channel, the companions, on the opposite, are always dim, $L_{\rm comp} \lesssim 0.1\,L_\odot$, and less massive than RR Lyrae. However, since both stars have relatively low masses, $M_{\rm RRL/comp} \lesssim 0.75\,M_\odot$, and due to a very broad period distribution, the majority of the binaries will have vanishing orbital velocities $v_{\rm orb,RRL/comp} \lesssim 1\,$km/s. Due to the short-period tail of the period distribution, about 10 per cent of the binary systems from the Single Channel may reach orbital velocities of $v_{\rm orb,RRL/comp} \lesssim 10\,$km/s.

Constructing an observational sample of binary companions to RR Lyrae requires one to overcome several challenges. Identifying composite RR Lyrae from a single spectrum is impossible for most systems because the companions are dimmer than RR Lyrae whilst not differing sufficiently in surface temperature. The systems with evolved companions on the RGB, shown in Figure 9, may be observed as composites. However, they need to be first identified as RR Lyrae despite their location away from the RR Lyrae clump

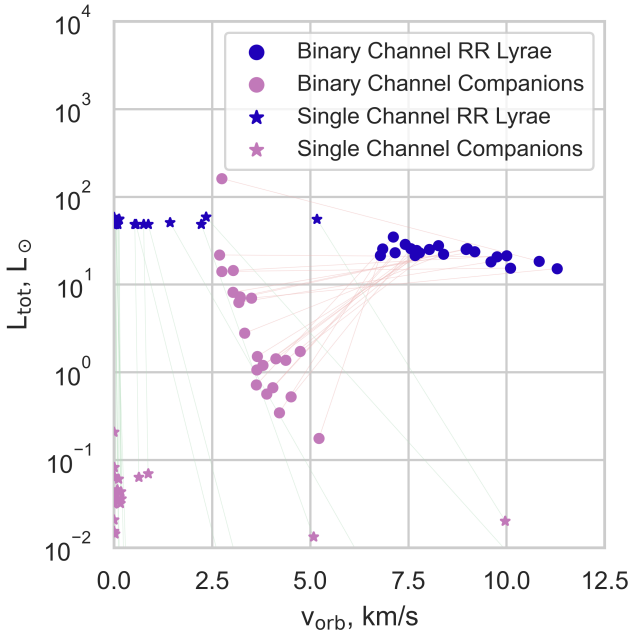

Figure 10. Orbital properties for binary RR Lyrae from the Single and Binary Channels. The horizontal axis shows the orbital velocities of both components, and the vertical axis shows their bolometric luminosities. The metal-rich RR Lyrae from the Binary Channel formed through binary stripping, and their companions are shown with circles. The classical old and metal-poor binary RR Lyrae from the Single Channel form effectively through single stellar evolution and are shown with star signs. One may see that the metal-rich RR Lyrae have bright companions, while most metal-poor RR Lyrae have relatively slow and several-magnitudes dimmer companions. Therefore, observing the classical metal-poor RR Lyrae companions from the Single Channel is more challenging than for the metal-rich RR Lyrae from the Binary Channel.

on the colour-magnitude diagram. Likewise, because of their small orbital velocities (and yet smaller radial velocities) and because the RR Lyrae pulsations themselves lead to spectral velocity shifts of the order of 50 km/s (Gillet et al. 2019), disentangling both spectral components of binary RR Lyrae from a mid- or high-resolution spectral series is also challenging. Additionally, such disentanglement requires spacing the spectral series over 2.7 – 4.8 years to cover the complete orbits of the systems. If disentangled, similar to the observed companions of sdB binaries (Vos et al. 2020), non-convective companions of metal-rich RR Lyrae will be enriched with CNO products from the preceding accretion from an evolved red giant, the RR Lyrae progenitor. Due to their wide orbits, binary RR Lyrae are also good targets for *Gaia* DR3 and subsequent *Gaia* data releases providing orbital solutions, with a possible caveat that the RR Lyrae variability may complicate the *Gaia* orbital solution. The binary period distribution in the current *Gaia* DR3 dataset only reaches up to about 1000 d (Gaia Collaboration et al. 2022), which is the lower end of the expected period distribution for binary RR Lyrae. Therefore, the current and future *Gaia* data releases may potentially probe the lower end of the period distribution for binary RR Lyrae. With the above challenges in mind, the current most yielding source of binary RR Lyrae, perhaps, may still be the existing candidate search techniques mentioned in Section 1 that include the light time travel effect, astrometric anomalies, radial velocities, eclipses and imaging.

3.4 Galactic Orbits and Rates

In Table 1, we present the Galactic population and formation rates of RR Lyrae from the Single and Binary Channels shown in Figure 2, as follows from our modelling. At present, the Galaxy contains 523 400 and 58 500 RR Lyrae from the Single and Binary Channels, respectively.

RR Lyrae from the Single Channel dominate the Galactic population making about 90 % of the Galactic RR Lyrae. In the fiducial model, all the RR Lyrae from the Single Channel are located in the Galactic Halo. However, as we discuss further in Section 4, the RR Lyrae from the Single Channel may be distributed between the Halo and the Thick Disc depending on the prescription for wind mass loss on the RGB. Under a plausible variation of wind mass loss parameters, the Galactic number of RR Lyrae from the Single Channel varies by no more than about 50 %. Finally, 38 % of the RR Lyrae from the Single Channel have a binary companion with a typically large orbital period. In such binaries, the RR Lyrae progenitor did not interact with the companion during the red giant phase, evolving effectively as a single star.

The RR Lyrae from the Binary Channel account for about 10 % of all the Galactic RR Lyrae. However, these systems make up for *all* the young and metal-rich RR Lyrae in our models. Furthermore, the young and metal-rich RR Lyrae from the Binary Channel dominate the RR Lyrae population in the Solar neighbourhood, making more than 70 % of RR Lyrae within a 500 pc radius around the Sun. The Binary Channel has such a significant local contribution because most of the systems from the Binary Channel reside in the Galactic Thin Disc, which is much more concentrated than the Halo populated by the RR Lyrae from the Single Channel.

About 10500 out of 58500 RR Lyrae from the Binary Channel reside in the Bulge. This is because the turn-off stars in the Bulge have masses $M_{\rm TO,bulge} \gtrsim 1.0\,{\rm M}_\odot$ and require stripping to land in the IS. For similar reasons, in our models, the Binary Channel produces no RR Lyrae in the Thick Disc. In other words, the Thick Disc contains no more than a few per cent of the RR Lyrae population from the Binary Channel. This may be understood since the majority of stars in the Thick Disc are old and metal-poor. Therefore, they have a turn-off mass that is just about appropriate to produce RR Lyrae through single stellar evolution. Consequently, it is harder for such stars to end up in the IS after binary interactions than for the more massive progenitors from the Thin Disc or the Bulge. Finally, another characteristic feature of RR Lyrae from the Binary Channel is that they live approximately 70 % longer than RR Lyrae from the Single Channel. This difference is because the RR Lyrae in the Halo evolve faster due to their much lower metallicity compared to Thin Disc stars.

Altogether, as we discuss in Section 4, the RR Lyrae from the Single Channel are consistent with the observed population of Classical RR Lyrae. At the same time, the RR Lyrae from the Binary Channel are compatible with the observations of RR Lyrae in the Thin Disc and the Bulge.

4 DISCUSSION

4.1 The Current Population of Binary RR Lyrae

In this study, we show that binary RR Lyrae from the Binary Channel presented in Figure 2 offer a natural explanation for the young and metal-rich population of RR Lyrae in the Thin Disc and Bulge. These RR Lyrae are abundant in the Galaxy and form a natural part of the population of binary stripped stars. Their surface temperatures

Type	Thin disc	Thick disc	Bulge	Halo	Total
R_{tot}, kyr^{-1}	0 : 0.51	0 : 0	0 : 0.13	9.46 : 0	9.46 : 0.63
N_{tot}	0 : 48 000	0 : 0	0 : 10 500	523 400 : 0	523 400 : 58 500
n_{loc}, kpc^{-3}	0 : 43.6	0 : 0	0 : 0	9.2 : 0	9.2 : 43.6
$N_{500\,pc}$	0 : 13.2	0 : 0	0 : 0	4.8 : 0	4.8 : 13.2
$N_{1\,kpc}$	0 : 70.5	0 : 0	0 : 0	38.4 : 0	38.4 : 70.5

Table 1. The Galactic populations and rates of the RR Lyrae in the Single and Binary Channels, as follows from our models. The entries in the table are given in the following format: 'Value for the Single Channel : Value for the Binary Channel'. The columns list the contributions from the main Galactic components: the Thin and Thick Discs, Bulge, Halo, and the Galactic Total. The rows show the present-day formation rate, the total number of systems, the local number density, and the number of systems in the 500 pc and 1 kpc neighbourhood of the Sun, for each of the Galactic components. The young and metal-rich Binary Channel contributes approximately 10 % of the total number of RR Lyrae in the Galaxy. In contrast, this same channel dominates the local density of RR Lyrae in the solar neighbourhood, making approximately an 82 % fraction since the Thin Disc hosting the Binary Channel is more concentrated than the old and metal-poor Halo containing the systems from the Single Channel. In the old metal-poor Single Channel, 38 % of stars have a large-period binary companion and underwent 'Effectively Single' evolution. As we discuss in Section 4, the fraction of RR Lyrae from the Single Channel in the Thick Disc and Halo may vary under a plausible variation of the wind mass loss model on the RGB. However, the total number of systems from this channel varies by less than about 50 %.

Catalogue	N_{match}	N_{clean}	$f_{disc/halo}$	$f_{rich/poor}$	$f_{disc/halo,control}$	$f_{rich/poor,control}$
RR Lyrae yrBinCan† (Liška et al. 2016a)	68	22	0.24 (4:17)	0.5 (10:20)	0.34	0.32
Hajdu et al. (2021)	63	3	0 (0:3)	0.28 (2:7)	0.34	0.32
Kervella et al. (2019a)	139	73	0.6 (27:45)	0.27 (18:67)	0.34	0.32
Kervella et al. (2019b)	7	3	2 (2:1)	2 (2:1)	0.73	0.46
Prudil et al. (2019)	8	1	0 (0:1)	0 (0:1)	0.46	0.30

Table 2. Fraction of disc-to-halo and metal-rich-to-metal poor stars in catalogues obtained from cross-matching the *Gaia* DR2 RR Lyrae catalogue (Iorio & Belokurov 2021) with catalogues of candidate RR Lyrae in binary systems: the online database RR Lyrae yrBinCan (Candidates for Binaries with an RR Lyrae Component database RR Lyrae yrBinCan, Liška et al. 2016a); the Hajdu et al. (2021) and Prudil et al. (2019) catalogues of candidates based on the light-travel time effect; the Kervella et al. (2019a) and Kervella et al. (2019b) dataset based on the proper motion anomaly and proper motion pairs. The first two columns indicate the number of matched stars (1 arcsec search window) and the number of stars matched that are also in the clean catalogue used in Iorio & Belokurov (2021). The third column represents the disc-to-halo stars ratio; the value in parenthesis is the number of stars associated with the (Thin) Disc and the Halo. The classification is based on the method described in Iorio & Belokurov (2021). The fourth column represents the metal-rich to metal-poor stars ratio. The metal-poor/metal-rich boundary is set at $[Fe/H] = -1$ and the metallicities are from the Iorio & Belokurov (2021) catalogue. The last two columns indicate the disc to halo and metal-rich to metal-poor ratios estimated in the *Gaia* DR2 RR Lyrae catalogue in the same Galactic region sampled by the cross-matched catalogue.

lie inside the broad continuum of the temperatures occupied by the observed populations of stripped core-helium burning stars. Therefore, the presence of binary RR Lyrae is insensitive to stellar modelling. Furthermore, the formation rates of RR Lyrae from the Binary Channel are comparable to those from the classical Single Channel in the Galaxy overall and even dominate the rates in the solar neighbourhood. Detecting and characterising such binary RR Lyrae systems, as we describe in Section 4.4, will lead to significant novel constraints on binary stellar evolution and, potentially, binary populations in the Galaxy.

The current biggest observational evidence for our modelled population of binary RR Lyrae lies in the large observed population of RR Lyrae in the metal-rich and Thin Disc environments, as mentioned in Section 1, and the good agreement between our models and their observed photometric properties, metallicities and formation rates.

In Table 2, we show the result of cross-matching the *Gaia* DR2 RR Lyrae catalogue in Iorio & Belokurov (2021) with several catalogues of binary RR Lyrae candidates. Despite the relatively large number of matches, only a small fraction of them belongs to the clean catalogue by Iorio & Belokurov (2021) for which we have a good metallicity estimate and a clear association to the Galactic disc. Almost all the matches with the clean catalogue come from the RR Lyrae yrBinCan database (Liška et al. 2016a) and the Kervella et al. (2019a) catalogue based on proper motion anomalies. Within these two catalogues, there are hints that binary candidates could be more common in the disc and/or the metal-rich RR Lyrae population. However, given the low statistics, it is not currently possible to derive any definite conclusion. We also tried to cross-match the Iorio & Belokurov (2021) dataset with the binary catalogues from *Gaia* DR3 (Halbwachs et al. 2022; Gaia Collaboration et al. 2022), but only four stars are inside the matching window (1 arcsec, considering the stars' proper motions). Considering the RR Lyrae catalogue from *Gaia* DR3 (Clementini et al. 2022), we found 11 matches with the DR3 binary catalogues: 10 in the `nss_two_body_orbit` table (consistent with orbital two-body solutions) and 1 in the `nss_acceleration_astro` (astrometric solutions consistent with non-linear proper motions). Among the 10 objects consistent with two-body orbit models: 4 are eclipsing binaries with periods twice the pulsation periods, and hence they are likely misclassified RRc RR Lyrae; 5 have spectroscopic solutions (SB1, see Gaia Collaboration et al. 2022) of which 4 have periods consistent with RR Lyrae pulsation, and thus they are likely spurious solutions biased by the intrinsic variability, the other one has a period of 14 days. The most interesting object is an RRc star (*Gaia* DR3 ID 5239771349915805952) consistent with a binary astrometric solution having a period 2287 ± 312 days[5].

It should be remembered that a 38 % fraction of the old and low-metallicity RR Lyrae from the Single Channel also has binary companions. The progenitors of such RR Lyrae started on sufficiently wide orbits so that they did not interact with the binary companion during the RGB and evolved effectively as single stars. The binary companions of effectively single RR Lyrae have a broad

[5] This object has been classified as a main sequence variable (BY Dra Variable) in Samus' et al. (2017)

period distribution spanning over several dex and reaching down to about 500 d.

One may potentially distinguish some of the binary RR Lyrae from the Binary and Effectively Single channels based on their eccentricity distributions. Indeed, RR Lyrae from the Effectively Single Channel preserve their birth eccentricity distribution, which is close to thermal ($\mathrm{d}N/\mathrm{d}e = 2e$). In comparison, the progenitors of RR Lyrae from the Binary Channel are likely circularised by mass transfer, and one might expect them to become circular and distinct from Single RR Lyrae. However, the observed stripped core-helium burning stars show mild eccentricities $e \lesssim 0.5$, most likely caused by the interaction with a circumbinary disc forming during mass transfer, e.g. Vos et al. (2015); Oomen et al. (2020). Therefore, RR Lyrae from both channels have non-zero eccentricity distributions. The distinguishing feature of the binary RR Lyrae from the Effectively Single Channel may be extreme eccentricities $e \gtrsim 0.6$ that may be impossible to reach within the Binary Channel, e.g. Vos et al. (2017). In addition to these effects, even a low-mass triple companion may further modify the eccentricity of the inner binary.

Observationally confirming binary companions for such stars is challenging. As we show in Section 3, for the majority of systems, the wide-orbit companions are relatively faint and have a similar temperature to RR Lyrae. Therefore, a several-year-long sequence of spectroscopic observations, similar in duration to the orbital periods of the systems, may be needed to disentangle the spectra and the RR Lyrae pulsations. One difficulty is that the pulsations themselves may significantly influence the spectra. In addition, the time travel effect in RR Lyrae, as e.g. used in Prudil et al. (2019); Hajdu et al. (2021), may be used to identify new binary candidates, along with the other methods mentioned in Section 1. The biggest contribution to the number of confirmed binary RR Lyrae may come from future *Gaia* observations, for which several year-long periods are optimal for detection.

As we also discussed in Section 3, a nearly 10 % fraction of RR Lyrae from the Binary Channel are expected to have an evolved companion so that the stars photometrically away from the IS can exhibit RR Lyrae pulsations. Similar systems can form in 0.3 % of cases through the Single Channel, and in 0.03 % of cases for the Single Channel may even form binaries where both components are RR Lyrae. Such systems may have already been detected, and identifying them will be valuable for stellar evolution as they have a well-constrained evolutionary path.

RR Lyrae with a white dwarf (WD) companion should not be uncommon either. In the Single Channel, the RR Lyrae progenitor may be the second most massive star in the binary, given that the binary is sufficiently wide initially. Therefore, by the time the secondary star becomes RR Lyrae, the primary may have completed its evolution and become a WD. As a result, as follows from our population modelling, approximately 15 % of binary RR Lyrae from the 'Effectively Single Channel' have a binary WD companion. In comparison, young and metal-rich RR Lyrae from the Binary Channel need to have relatively massive WD companions $M_{\mathrm{WD}} \gtrsim 0.8\,\mathrm{M}_{\odot}$ in order to form through stable mass transfer (lower-mass WD companions will typically lead to a common envelope phase). Therefore, only approximately 1 % of the young and metal-rich RR Lyrae may have a WD companion.

4.2 Comparison with Previous Results

Our study builds on the Karczmarek et al. (2017) study that identified multiple possible channels of producing binary RR Lyrae pulsators. We focussed on the systems formed through helium flash since they are closest structurally to the classical RR Lyrae and have similar core masses and surface temperatures. Unlike Karczmarek et al. (2017), we found that such systems make a significant fraction of all the Galactic RR Lyrae and can fully explain the population of young and metal-rich RR Lyrae. Compared to Karczmarek et al. (2017), we used a detailed stellar structure code, which is important for modelling He ignition (Vos et al. 2020), a standard binary mass transfer model and a standard observationally-motivated Galactic population of binaries. Other channels identified in Karczmarek et al. (2017) should be similarly studied with detailed stellar evolution codes in the future. However, based on their analysis, these channels should make a small relative contribution to the overall population of binary RR Lyrae.

4.3 Caveats

The existence of binary metal-rich RR Lyrae in the Galactic disc is a robust prediction of binary stellar evolution calibrated by observations of related systems. While binary companions of metal-rich RR Lyrae in the disc are still to be confirmed, we review below the possible caveats for our study.

4.3.1 Stellar Winds

At very high metallicities, $[\mathrm{Fe/H}] \gtrsim -0.5$, low-mass core-helium-burning stars have too low surface temperatures, and they cluster on the so-called red clump. The only way to move these stars toward the instability strip is to postulate a significant amount of mass loss on the RGB (see, e.g. Bono et al. 1997a,b). Bono et al. (1997a,b) postulated that young metal-rich RR Lyrae can be produced by progenitors with an initial mass within $1 - 2\,\mathrm{M}_{\odot}$ that have lost a considerable amount of mass during the ascent of the RGB ($M_{\mathrm{lost}} > 0.5\,\mathrm{M}_{\odot}$). Although there is evidence of mass-loss enhancement for metal-rich low-mass population II stars in the Bulge (Savino et al. 2020) and some globular clusters (Tailo et al. 2020), the mass lost during the RGB is constrained to be lower than $0.3\,\mathrm{M}_{\odot}$ (Gratton et al. 2010; Salaris et al. 2013; Origlia et al. 2014; Savino et al. 2018, 2019, 2020; Tailo et al. 2020, 2022). The amount of mass loss required to form such young and metal-rich RR Lyrae stars can be reduced assuming significant helium enrichment (Marsakov et al. 2019). Helium-enriched stars are likely observed in the so-called second-generation populations in globular clusters (Tailo et al. 2020; Dondoglio et al. 2021) and the Bulge (Minniti 1995). Still, there is no evidence of such stars in the Milky Way disc(s) (Reddy et al. 2006; Karakas 2014) or He-enriched RR Lyrae stars in the Bulge (Marconi & Minniti 2018). Therefore, the Bono et al. (1997a,b) scenario is in tension with the observational constraints on RGB mass loss in non-He-enriched environments.

The amount of envelope retained at the end of the RGB phase is a key criterion for producing RR Lyrae stars. The wind mass loss along the RGB is usually parameterised following Kudritzki & Reimers (1978):

$$\dot{M}_{\mathrm{RGB}} = \eta \times 4 \times 10^{-13} \times \left(\frac{L}{\mathrm{L}_{\odot}}\right)\left(\frac{M}{\mathrm{M}_{\odot}}\right)\left(\frac{R}{\mathrm{R}_{\odot}}\right)^{-1} \mathrm{M}_{\odot}\,\mathrm{yr}^{-1}, \qquad (2)$$

where L, M and R are the bolometric stellar luminosity, the stellar mass and radius, and η is the normalisation factor. The MIST tracks used in this work (Section 3.1) have been computed using $\eta = 0.1$. Consequently, just a tiny amount of mass is lost along the RGB (0.030-0.036 $\mathrm{M}_{\odot}$). Typical η values found in literature range

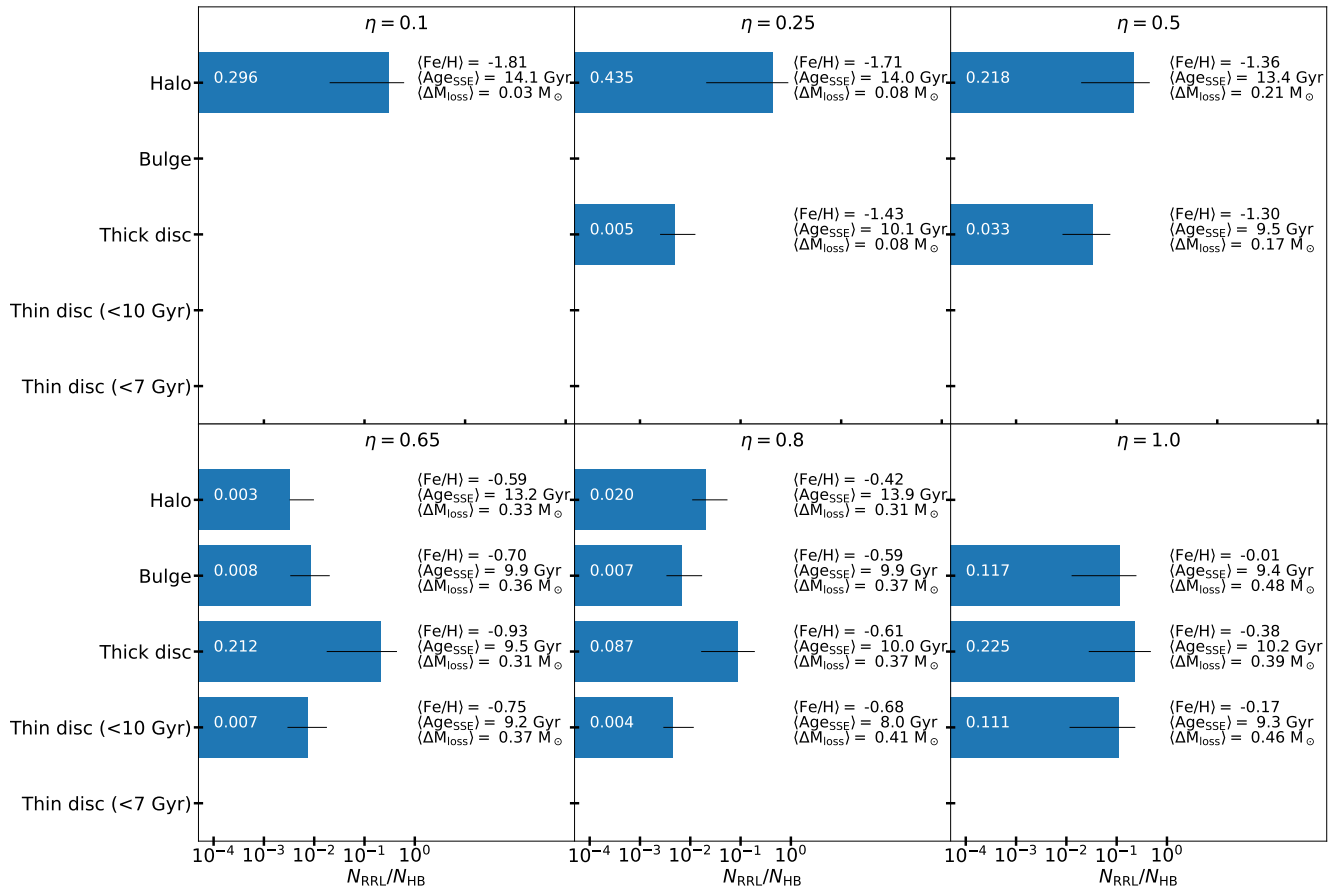

Figure 11. Number ratio between the objects in the instability strip and the stars currently burning helium in the core considering single stellar evolution only. The panels show the results obtained with different assumptions on the wind mass loss parameter η (Equation 2), while each bar refers to a given Galactic component (see Section 2.2). The values on the right indicate the average metallicity $\langle$Fe/H$\rangle$, age $\langle \mathrm{Age_{SSE}} \rangle$ and mass lost in the RGB $\langle \Delta \mathrm{M_{loss}} \rangle$ for the population of RR Lyrae stars in each Galactic component. The stellar evolution in this figure has been modelled using the population synthesis code MOBSE (Giacobbo et al. 2018; Giacobbo & Mapelli 2018, see Section 4.3.1).

between 0.1 and 0.6 and the amount of mass lost seems to increase with metallicity (Gratton et al. 2010; Lei et al. 2013; Miglio et al. 2013; Origlia et al. 2014; McDonald & Zijlstra 2015; Savino et al. 2019, 2020; Tailo et al. 2020, 2021).

To analyse the impact of mass-loss on the formation of RR Lyrae, we evolve a sample of stars using the public version of the population synthesis code MOBSE[6] (Giacobbo et al. 2018; Giacobbo & Mapelli 2018). For each Galactic component, we have drawn 10^5 stars sampling the initial masses, ages and metallicities as described in Section 2.2, and then the stars are evolved up to the current time (14 Gyr). We replicate this analysis for 6 different values of η: 0.1, 0.25, 0.5, 0.65, 0.8, 1.0. In Figure 11, we show the RR Lyrae formation efficiency as the ratio between the stars in the instability strip and all the stars that are currently burning helium in the core. For $\eta = 0.1$, only old and metal-poor Halo stars can enter the instability strip, confirming what we found with the MIST stellar tracks (Section 3.1). For larger values of the wind mass loss parameter ($\eta = 0.25 - 0.5$), the RR Lyrae population is composed of the Halo and Thick Disc stars. At $\eta = 0.25$ the halo-to-disc formation efficiency ratio (≈ 100) is consistent with the one estimated by Layden (1995b) in the solar neighbourhood. Mass loss is significantly enhanced for more extreme values of η, and the stars lose from 0.3 up to 0.48 $\mathrm{M_\odot}$ during the RGB. In this case, the RR Lyrae can also be produced in the Bulge and in the old portion of the Thin Disc (> 7 Gyr). At the same time, the Halo population is composed just of the few stars in the metal-rich tail. Therefore, no single value of η can produce a realistic population of both metal-rich RR Lyrae and RR Lyrae in the Halo.

We further consider the possibility that the wind parameter η increases sufficiently for higher-metallicity stars to produce a population of metal-rich RR Lyrae. Indeed, high values of η can quite efficiently produce RR Lyrae in almost all the Galactic components. However, some necessary cautions are needed in the interpretation of such results. First, the relation between η and the effective amount of mass lost depends on the assumed stellar evolution tracks. Tailo et al. (2020) found that high values of η (up to 0.65 – 0.7) are required to explain the horizontal branch of the most metal-rich globular clusters (GCs). However, the maximum mass lost in their model is 0.3 $\mathrm{M_\odot}$. This value is consistent with $\eta < 0.6$ in the MOBSE stellar models. In addition, it is important to stress that most of the analysed metal-rich ([Fe/H] > −1) GCs in the Tailo et al. (2020) sample are devoid of RR Lyrae (NGC5927 Liller 1983; NGC6352, Alcaino 1971; NGC6496, Abbas et al. 2015; NGC6838,

[6] https://mobse-webpage.netlify.app

McCormac et al. 2014) or contain few candidates that are likely interlopers (47Tuc, Bono et al. 2008; NGC6304, De Lee et al. 2006; NGC 6366, Arellano Ferro et al. 2008; NGC6624, Liller & Carney 1978; NGC6367, Escobar et al. 2006). The only metal-rich GC in the sample containing several confirmed RR Lyrae members is NGC 6441, for which an integrated mass loss of $\approx 0.25\,M_\odot$ is required ($\eta \approx 0.5$). However, the RR Lyrae in this GC are peculiar objects with long periods consistent with the metal-poor population of field RR Lyrae (Alonso-García et al. 2021; Pritzl et al. 2000). Figure 11 also shows that for $\eta = 0.65$ the formation efficiency in the Thick Disc is comparable with the formation efficiency for the stellar Halo at $\eta < 0.65$. Given the large mass difference between the two components ($M_{\rm thick-disc}/M_{\rm halo} > 15$), a large value of η at the metallicity of the Thick Disc implies that the observed RR Lyrae stars should be mostly in the Thick Disc. Therefore, even the model with a varying wind parameter η is inconsistent with the Galactic distribution of RR Lyrae.

Finally, Figure 11 clearly shows that no truly young population of RR Lyrae (< 7 Gyr) can be produced through the Single Channel. Therefore, we can conclude that independently of the RGB wind-mass loss uncertainties, the Single Channel alone cannot explain the observed populations of young and metal-rich RR Lyrae stars.

4.3.2 *Pulsation Properties*

The Binary Channel of RR Lyrae can place core-helium burning stars in the instability strip because binary stripping can reduce the envelope mass of red metal-rich HB stars and make them hotter. While both single and binary RR Lyrae undergo a He flash at nearly identical core mass distributions, their hydrogen envelope masses and metallicities differ. In particular, single RR Lyrae typically have cores of $0.495 - 0.515\,M_\odot$ and envelopes of $0.22 - 0.24\,M_\odot$. In comparison, binary RR Lyrae have cores of $0.460 - 0.475\,M_\odot$ and envelopes of $0.04 - 0.07\,M_\odot$. Given that the RR Lyrae pulsation mechanism relies on the partial ionisation of helium, it appears reasonable that the pulsation lightcurves should not depend significantly on the envelope mass. However, detailed asteroseismic modelling is needed to determine the pulsation profiles of such stars. Even more so, a detailed study is necessary to model the population and properties of the pulsators that ignited helium non-degenerately not included in this study (see, e.g. Smolec et al. 2013; Chadid et al. 2017).

Lastly, the answer to a general question of how a stellar pulsator emerges from the preceding binary mass transfer episode and whether such pulsations may interfere with mass transfer is, as of yet, not known and is worth studying.

4.3.3 *Binary Periods*

Another possible caveat of our model is the final orbital periods of RR Lyrae. It is known that periods resulting from binary mass transfer are sensitive to mass and angular momentum loss (Soberman et al. 1997). While the observed population of long-period sdB stars strongly constrains mass loss to be significantly non-conservative, the final orbital periods of sdB stars have no sensitivity to the angular momentum loss (Chen et al. 2013; Vos et al. 2020). Therefore, if the formation of binary RR Lyrae is sensitive to angular momentum loss, their orbital periods may change. Conversely, if this is the case, measuring the orbital periods of RR Lyrae may put novel constraints on the angular momentum loss in binary evolution. Finally, independently of the angular momentum loss model, the population of RR Lyrae from the Binary Channel is robustly produced since these stars lie within the well-constrained continuous temperature distribution of binary stripped stars.

4.3.4 *Observed RR Lyrae Stars in Binary Systems*

The final caveat is that the two currently confirmed binary RR Lyrae come from channels different from the Binary Channel, which was the main focus of this study. In particular, the OGLE-BLG-RR Lyrae YR-02792 object has a mass of $0.26\,M_\odot$ and cannot be produced by any of the channels we considered. The detection of such an object is likely enabled by its short 15 d period, to which binary microlensing detections are biased. Therefore, OGLE-BLG-RR Lyrae YR-02792 may represent a rarer but easier detectable population from one of the channels described in Karczmarek et al. (2017), e.g. RR Lyrae from the more massive progenitors than considered here ($M_{\rm progenitor} \gtrsim 2.1\,M_\odot$) that ignited helium non-degenerately.

The other confirmed binary RR Lyrae TU UMa has Halo kinematics and, given its $\approx$ 8000 d orbital period, is most certainly from the 'Effectively Single Channel'. Indeed, as follows from Section 3.4, all the binary RR Lyrae in the Halo and 73 % of all the binary RR Lyrae in the Galaxy come from the 'Effectively Single Channel'. Therefore, it is expected that the only confirmed long-period binary RR Lyrae also comes from this channel. Conversely, as follows from Section 3, any binary metal-rich RR Lyrae should expectedly have companions with several times shorter orbital periods of 1000 – 2000 d. Generally, any further observational limits on the formation rates and period distribution of long-period binary RR Lyrae will be highly constraining for the models of these systems.

4.4 Implications

The main implication of this study is that metal-rich RR Lyrae in the Thin Disc and Bulge represent a young (< 7 GyR) stellar population. In particular, metal-rich RR Lyrae, the dominant RR Lyrae flavour in the solar neighbourhood, cannot serve as age indicators or tracers of old stellar populations. Conversely, the presence or absence of metal-rich RR Lyrae in a given sample may inform the Galactic population studies.

RR Lyrae as distance indicators should also be used with caution. While the metal-rich RR Lyrae are consistent with the (period)-luminosity-metallicity relation, their binary origins call for a more detailed study of their pulsations. In particular, the pulsation lightcurves may differ from those predicted by wind mass loss models for the classical RR Lyrae from the Single Channel. Furthermore, since metal-rich RR Lyrae have a notably lower luminosity than metal-poor RR Lyrae, the mean metallicity estimates for a given sample may be biased, especially when one considers the Disc and Halo regions of other galaxies, potentially leading to biased distance estimates.

With their future characterisation, binary RR Lyrae will join the long- and short- period sdB binaries as the primary probes of the red giant mass transfer. All three populations may be modelled in detail within the same theoretical framework. Together with the mass distribution of short-period sdB binaries, observed periods of binary RR Lyrae can potentially put novel constraints on the angular momentum loss in RG-MS binaries. The absence of short-period RR Lyrae may be used to constrain common envelope evolution.

The Binary Channel explored in this study may be especially important for modelling RR Lyrae in dynamical environments such

as globular clusters or nuclear star clusters, where dynamical collisions may lead to stripping thus producing binary RR Lyrae as studied here. Disentangling the primordial and binary populations of RR Lyrae can be potentially used as a probe of their globular cluster hosts, see, e.g. Davies et al. (2004).

The existence of RR Lyrae produced in binaries implies that there are several related populations. In particular, the binaries with more massive A- and B-type accretors may lead to Be stars in binaries with RR Lyrae similar to the observed Be-sdO/B stars, e.g. Wang et al. (2021). Furthermore, since a non-negligible fraction of field binaries are members of triple systems, e.g. Toonen et al. (2016), a subset of binary RR Lyrae will have a triple stellar companion, which may potentially provide unique prospects for characterising such systems through timing. Finally, as we showed in Section 3, since binary RR Lyrae may be produced from progenitors with initial mass ratios close to unity, some RR Lyrae will have an evolved binary companion, and more rarely, another RR Lyrae in the same binary. And conversely, the absence of such systems may constrain the evolution of nearly equal mass binaries. For the same reason, a small fraction of binary RR Lyrae may be found with exotic companions, such as CO/ONe white dwarfs or neutron stars. Finally, similar mass transfer processes are relevant for forming the more massive cepheid-like variables with possible implications for cosmology, e.g. see Karczmarek et al. (2022).

Interestingly, there are several confirmed binary systems containing a δScuti variable (Liakos & Niarchos 2017; Kahraman Aliçavuş et al. 2017; Guzik 2021; Kahraman Alicavus et al. 2022). Therefore, some of the progenitors of metal-rich RR Lyrae from the Binary Channel with masses between $1.5 - 2.5\,M_\odot$, see Figure 7, cross the instability strip also during the main sequence. Such stars could be detected as low-period pulsators such as δScuti or γDoradus stars (Sánchez Arias et al. 2018). Therefore, a certain fraction of δScuti+MS binaries will become pulsators once again once they turn into RR Lyrae.

ACKNOWLEDGEMENTS

G.I. and V.B. are grateful to C. Tout for the illuminating discussion that kicked off this project. G.I. thanks Guglielmo Costa for interesting and stimulating discussions and for the inclusion of the MIST tracks in SEVN. A.B. acknowledges support for this project from the European Union's Horizon 2020 research and innovation program under grant agreement No. 865932-ERC-SNeX. The MESA simulations were performed on the resources provided by the Swedish National Infrastructure for Computing (SNIC) at the Lunarc cluster. J.V. acknowledges support from the Grant Agency of the Czech Republic (GAČR 22-34467S). The Astronomical Institute Ondřejov is supported by the project RVO:67985815. G.I. acknowledges financial support from the European Research Council for the ERC Consolidator grant DEMOBLACK, under contract no. 770017. G.I. and V.B. acknowledge support for this project by the Newton International Fellowship Alumni follow-on funding (2020, AL201003). G.I. thanks the Simons Foundation for financial support during his visit at the CCA where part of this work was performed.

DATA AVAILABILITY

The data underlying this article will be shared on reasonable request to the corresponding authors.

REFERENCES

Abbas M. A., et al., 2015, AJ, 149, 40
Ablimit I., Zhao G., Flynn C., Bird S. A., 2020, arXiv e-prints, p. arXiv:2004.13768
Abt H. A., 1983, ARA&A, 21, 343
Alcaino G., 1971, A&A, 11, 7
Alonso-García J., et al., 2021, A&A, 651, A47
Arellano Ferro A., Giridhar S., Rojas López V., Figuera R., Bramich D. M., Rosenzweig P., 2008, Rev. Mex. Astron. Astrofis., 44, 365
Babusiaux C., et al., 2022, arXiv e-prints, p. arXiv:2206.05989
Barnes Thomas G. I., Guggenberger E., Kolenberg K., 2021, AJ, 162, 117
Bazan G., Mathews G. J., 1990, ApJ, 354, 644
Beaton R. L., et al., 2016, ApJ, 832, 210
Belczynski K., Kalogera V., Rasio F. A., Taam R. E., Zezas A., Bulik T., Maccarone T. J., Ivanova N., 2008, ApJS, 174, 223
Belokurov V., Kravtsov A., 2022, MNRAS, 514, 689
Belokurov V., Erkal D., Deason A. J., Koposov S. E., De Angeli F., Evans D. W., Fraternali F., Mackey D., 2017, MNRAS, 466, 4711
Belokurov V., Erkal D., Evans N. W., Koposov S. E., Deason A. J., 2018, MNRAS, 478, 611
Belokurov V., Sanders J. L., Fattahi A., Smith M. C., Deason A. J., Evans N. W., Grand R. J. J., 2020, MNRAS, 494, 3880
Bobrick A., Davies M. B., Church R. P., 2017, MNRAS, 467, 3556
Bono G., Caputo F., Cassisi S., Castellani V., Marconi M., 1997a, ApJ, 479, 279
Bono G., Caputo F., Cassisi S., Incerpi R., Marconi M., 1997b, ApJ, 483, 811
Bono G., et al., 2008, ApJ, 686, L87
Bovy J., Rix H.-W., Schlafly E. F., Nidever D. L., Holtzman J. A., Shetrone M., Beers T. C., 2016, The Astrophysical Journal, 823, 30
Braga V. F., et al., 2015, ApJ, 799, 165
Catelan M., 2004, in Kurtz D. W., Pollard K. R., eds, Astronomical Society of the Pacific Conference Series Vol. 310, IAU Colloq. 193: Variable Stars in the Local Group. p. 113 (arXiv:astro-ph/0310159)
Catelan M., 2009, Ap&SS, 320, 261
Catelan M., Smith H. A., 2015, Pulsating Stars
Chadid M., Sneden C., Preston G. W., 2017, ApJ, 835, 187
Chen X., Han Z., Deca J., Podsiadlowski P., 2013, MNRAS, 434, 186
Choi J., Dotter A., Conroy C., Cantiello M., Paxton B., Johnson B. D., 2016, ApJ, 823, 102
Clementini G., et al., 2022, arXiv e-prints, p. arXiv:2206.06278
Conroy C., et al., 2022, arXiv e-prints, p. arXiv:2204.02989
Crestani J., et al., 2021, ApJ, 914, 10
Cusano F., et al., 2021, MNRAS, 504, 1
Czekaj M. A., Robin A. C., Figueras F., Luri X., Haywood M., 2014, A&A, 564, A102
Davies M. B., Piotto G., de Angeli F., 2004, MNRAS, 349, 129
De Lee N., Catelan M., Layden A., Pritzl B., Smith H., Sweigart A., Welch D. L., 2006, Mem. Soc. Astron. Italiana, 77, 117
Deason A. J., Belokurov V., Sanders J. L., 2019, MNRAS, 490, 3426
Deschamps R., Siess L., Davis P. J., Jorissen A., 2013, A&A, 557, A40
Dondoglio E., Milone A. P., Lagioia E. P., Marino A. F., Tailo M., Cordoni G., Jang S., Carlos M., 2021, ApJ, 906, 76
Dotter A., 2016, ApJS, 222, 8
Escobar M. E., et al., 2006, in Revista Mexicana de Astronomia y Astrofisica Conference Series. p. 168
Fainer S., Bear E., Soker N., 2022, arXiv e-prints, p. arXiv:2204.12360
Feast M. W., Laney C. D., Kinman T. D., van Leeuwen F., Whitelock P. A., 2008, MNRAS, 386, 2115
Feuillet D. K., Feltzing S., Sahlholdt C., Bensby T., 2022, arXiv e-prints, p. arXiv:2206.03875
Fiorentino G., et al., 2015, ApJ, 798, L12
Fiorentino G., et al., 2017, A&A, 599, A125
Gaia Collaboration et al., 2022, arXiv e-prints, p. arXiv:2206.05595
Giacobbo N., Mapelli M., 2018, MNRAS, 480, 2011
Giacobbo N., Mapelli M., Spera M., 2018, MNRAS, 474, 2959
Gillet D., Mauclaire B., Lemoult T., Mathias P., Devaux J. S., de France T.,

Garrel T., 2019, A&A, 623, A109
Gilligan C. K., et al., 2021, MNRAS, 503, 4719
Gozha M. L., Marsakov V. A., Koval V. V., 2021, Astronomical and Astrophysical Transactions, 32, 147
Gran F., Minniti D., Saito R. K., Navarrete C., Dékány I., McDonald I., Contreras Ramos R., Catelan M., 2015, A&A, 575, A114
Gratton R. G., Carretta E., Bragaglia A., Lucatello S., D'Orazi V., 2010, A&A, 517, A81
Gravity Collaboration et al., 2018, A&A, 615, L15
Guzik J. A., 2021, Frontiers in Astronomy and Space Sciences, 8, 55
Hajdu G., Catelan M., Jurcsik J., Dékány I., Drake A. J., Marquette J.-B., 2015, Monthly Notices of the Royal Astronomical Society: Letters, 449, L113
Hajdu G., et al., 2021, ApJ, 915, 50
Halbwachs J.-L., et al., 2022, arXiv e-prints, p. arXiv:2206.05726
Han Z., Tout C. A., Eggleton P. P., 2000, MNRAS, 319, 215
Han Z., Podsiadlowski P., Maxted P. F. L., Marsh T. R., Ivanova N., 2002, MNRAS, 336, 449
Haschke R., Grebel E. K., Duffau S., 2011, AJ, 141, 158
Haywood M., Robin A. C., Creze M., 1997, A&A, 320, 428
Heber U., 2016, PASP, 128, 082001
Holl B., et al., 2018, preprint, (arXiv:1804.09373)
Hurley J. R., Tout C. A., Pols O. R., 2002, MNRAS, 329, 897
Iorio G., Belokurov V., 2019, MNRAS, 482, 3868
Iorio G., Belokurov V., 2021, MNRAS, 502, 5686
Iorio G., Belokurov V., Erkal D., Koposov S. E., Nipoti C., Fraternali F., 2018, MNRAS, 474, 2142
Jurić M., et al., 2008, ApJ, 673, 864
Kahraman Alicavus F., Gumus D., Kirmizitas O., Ekinci O., Cavus S., Kaya Y. T., Alicavus F., 2022, arXiv e-prints, p. arXiv:2204.12952
Kahraman Aliçavuş F., Soydugan E., Smalley B., Kubát J., 2017, MNRAS, 470, 915
Karakas A. I., 2014, MNRAS, 445, 347
Karczmarek P., Wiktorowicz G., Iłkiewicz K., Smolec R., Stępień K., Pietrzyński G., Gieren W., Belczynski K., 2017, MNRAS, 466, 2842
Karczmarek P., Smolec R., Hajdu G., Pietrzyński G., Gieren W., Narloch W., Wiktorowicz G., Belczynski K., 2022, ApJ, 930, 65
Kervella P., et al., 2019a, A&A, 623, A116
Kervella P., et al., 2019b, A&A, 623, A117
Kippenhahn R., Weigert A., Weiss A., 2013, Stellar Structure and Evolution, doi:10.1007/978-3-642-30304-3.
Kiss L. L., Szatmary K., Gal J., Kaszas G., 1995, Information Bulletin on Variable Stars, 4205, 1
Kroupa P., 2008, in Knapen J. H., Mahoney T. J., Vazdekis A., eds, Astronomical Society of the Pacific Conference Series Vol. 390, Pathways Through an Eclectic Universe. p. 3 (arXiv:0708.1164)
Kudritzki R. P., Reimers D., 1978, Mitteilungen der Astronomischen Gesellschaft Hamburg, 43, 263
Layden A. C., 1995a, AJ, 110, 2288
Layden A. C., 1995b, AJ, 110, 2312
Lei Z. X., Chen X. F., Zhang F. H., Han Z., 2013, A&A, 549, A145
Li L. J., Qian S. B., 2014, MNRAS, 444, 600
Li L. J., Qian S. B., Zhu L. Y., 2018, ApJ, 863, 151
Li J., et al., 2022a, arXiv e-prints, p. arXiv:2205.11734
Li X.-Y., Huang Y., Liu G.-C., Beers T. C., Zhang H.-W., 2022b, arXiv e-prints, p. arXiv:2206.07668
Liakos A., Niarchos P., 2017, MNRAS, 465, 1181
Liller M. H., 1983, AJ, 88, 404
Liller M. H., Carney B. W., 1978, ApJ, 224, 383
Liu S., Zhao G., Chen Y.-Q., Takeda Y., Honda S., 2013, Research in Astronomy and Astrophysics, 13, 1307
Liška J., Skarka M., Zejda M., Mikulášek Z., de Villiers S. N., 2016a, MNRAS, 459, 4360
Liška J., Skarka M., Mikulášek Z., Zejda M., Chrastina M., 2016b, A&A, 589, A94
Maintz G., de Boer K. S., 2005, A&A, 442, 229
Mapelli M., Spera M., Montanari E., Limongi M., Chieffi A., Giacobbo N., Bressan A., Bouffanais Y., 2020, ApJ, 888, 76
Marconi M., Minniti D., 2018, The Astrophysical Journal, 853, L20
Marsakov V. A., Gozha M. L., Koval V. V., 2018, Astronomy Reports, 62, 50
Marsakov V. A., Gozha M. L., Koval' V. V., 2019, Astronomy Reports, 63, 203
McCormac J., Skillen I., Pollacco D., Faedi F., Ramsay G., Dhillon V. S., Todd I., Gonzalez A., 2014, MNRAS, 438, 3383
McDonald I., Zijlstra A. A., 2015, MNRAS, 448, 502
McMillan P. J., 2011, MNRAS, 414, 2446
Miglio A., et al., 2013, MNRAS, 429, 423
Minniti D., 1995, A&A, 300, 109
Minniti D., et al., 1999, in Gibson B. K., Axelrod R. S., Putman M. E., eds, Astronomical Society of the Pacific Conference Series Vol. 165, The Third Stromlo Symposium: The Galactic Halo. p. 284
Moe M., Kratter K. M., Badenes C., 2019, ApJ, 875, 61
Monelli M., et al., 2018, MNRAS, 479, 4279
Mullen J. P., et al., 2021, ApJ, 912, 144
Muraveva T., Garofalo A., Scowcroft V., Clementini G., Freedman W. L., Madore B. F., Monson A. J., 2018a, MNRAS, 480, 4138
Muraveva T., Delgado H. E., Clementini G., Sarro L. M., Garofalo A., 2018b, MNRAS, 481, 1195
Muraveva T., Clementini G., Garofalo A., Cusano F., 2020, MNRAS, 499, 4040
Myeong G. C., Vasiliev E., Iorio G., Evans N. W., Belokurov V., 2019, MNRAS, 488, 1235
Myeong G. C., Belokurov V., Aguado D. S., Evans N. W., Caldwell N., Bradley J., 2022, arXiv e-prints, p. arXiv:2206.07744
Navarro M. G., Minniti D., Capuzzo-Dolcetta R., Alonso-García J., Contreras Ramos R., Majaess D., Ripepi V., 2021, A&A, 646, A45
Oomen G.-M., Pols O., Van Winckel H., Nelemans G., 2020, A&A, 642, A234
Origlia L., Ferraro F. R., Fabbri S., Fusi Pecci F., Dalessandro E., Rich R. M., Valenti E., 2014, A&A, 564, A136
Paczynski B., 1991, ApJ, 370, 597
Paxton B., Bildsten L., Dotter A., Herwig F., Lesaffre P., Timmes F., 2011, ApJS, 192, 3
Paxton B., et al., 2013, ApJS, 208, 4
Paxton B., et al., 2015, ApJS, 220, 15
Paxton B., et al., 2018, ApJS, 234, 34
Paxton B., et al., 2019, ApJS, 243, 10
Pérez-Villegas A., Portail M., Gerhard O., 2017, MNRAS, 464, L80
Pietrukowicz P., et al., 2015, ApJ, 811, 113
Pietrzyński G., et al., 2012, Nature, 484, 75
Popham R., Narayan R., 1991, ApJ, 370, 604
Pritzl B., Smith H. A., Catelan M., Sweigart A. V., 2000, ApJ, 530, L41
Prudil Z., Skarka M., Liška J., Grebel E. K., Lee C. U., 2019, MNRAS, 487, L1
Prudil Z., Dékány I., Grebel E. K., Kunder A., 2020, MNRAS, 492, 3408
Raghavan D., et al., 2010, ApJS, 190, 1
Reddy B. E., Lambert D. L., Allende Prieto C., 2006, MNRAS, 367, 1329
Richmond M. W., 2011, Journal of the American Association of Variable Star Observers (JAAVSO), 39, 201
Riess A. G., et al., 2016, ApJ, 826, 56
Robin A. C., Reylé C., Derrière S., Picaud S., 2003, A&A, 409, 523
Robin A. C., Marshall D. J., Schultheis M., Reylé C., 2012, A&A, 538, A106
Robin A. C., Reylé C., Fliri J., Czekaj M., Robert C. P., Martins A. M. M., 2014, A&A, 569, A13
Saha A., White R. E., 1990, PASP, 102, 148
Salaris M., de Boer T., Tolstoy E., Fiorentino G., Cassisi S., 2013, A&A, 559, A57
Salinas R., Hajdu G., Prudil Z., Howell S., Catelan M., 2020, Research Notes of the AAS, 4, 143
Samus' N. N., Kazarovets E. V., Durlevich O. V., Kireeva N. N., Pastukhova E. N., 2017, Astronomy Reports, 61, 80
Sánchez Arias J. P., Romero A. D., Córsico A. H., Pelisoli I., Antoci V., Kepler S. O., Althaus L. G., Corti M. A., 2018, A&A, 616, A80
Sarajedini A., Barker M. K., Geisler D., Harding P., Schommer R., 2006, AJ, 132, 1361

Savino A., de Boer T. J. L., Salaris M., Tolstoy E., 2018, MNRAS, 480, 1587
Savino A., Tolstoy E., Salaris M., Monelli M., de Boer T. J. L., 2019, A&A, 630, A116
Savino A., Koch A., Prudil Z., Kunder A., Smolec R., 2020, A&A, 641, A96
Schlafly E. F., Finkbeiner D. P., 2011, ApJ, 737, 103
Schönrich R., 2012, MNRAS, 427, 274
Schönrich R., Binney J., Dehnen W., 2010, MNRAS, 403, 1829
Sesar B., et al., 2014, ApJ, 793, 135
Sharma S., et al., 2020, arXiv e-prints, p. arXiv:2004.06556
Smith H. A., 2004, RR Lyrae Stars
Smolec R., et al., 2013, MNRAS, 428, 3034
Soberman G. E., Phinney E. S., van den Heuvel E. P. J., 1997, A&A, 327, 620
Soszyński I., et al., 2009, Acta Astron., 59, 1
Soszyński I., et al., 2011, Acta Astron., 61, 1
Spera M., Mapelli M., 2017, MNRAS, 470, 4739
Spera M., Mapelli M., Giacobbo N., Trani A. A., Bressan A., Costa G., 2019, MNRAS, 485, 889
Szeidl B., Olah K., Mizser A., 1986, Commmunications of the Konkoly Observatory Hungary, 89, 57
Tailo M., et al., 2020, MNRAS, 498, 5745
Tailo M., et al., 2021, MNRAS, 503, 694
Tailo M., et al., 2022, arXiv e-prints, p. arXiv:2205.06645
Tauris T. M., van den Heuvel E. P. J., 2006, Formation and evolution of compact stellar X-ray sources. pp 623–665
Toonen S., Hamers A., Portegies Zwart S., 2016, Computational Astrophysics and Cosmology, 3, 6
Torrealba G., et al., 2019, MNRAS, 488, 2743
Tout C. A., Eggleton P. P., 1988, MNRAS, 231, 823
Vos J., Østensen R. H., Marchant P., Van Winckel H., 2015, A&A, 579, A49
Vos J., Østensen R. H., Vučković M., Van Winckel H., 2017, A&A, 605, A109
Vos J., Vučković M., Chen X., Han Z., Boudreaux T., Barlow B. N., Østensen R., Németh P., 2019, MNRAS, 482, 4592
Vos J., Bobrick A., Vučković M., 2020, A&A, 641, A163
Wade R. A., Donley J., Fried R., White R. E., Saha A., 1999, AJ, 118, 2442
Wang L., Gies D. R., Peters G. J., Götberg Y., Chojnowski S. D., Lester K. V., Howell S. B., 2021, AJ, 161, 248
Zinn R., Chen X., Layden A. C., Casetti-Dinescu D. I., 2020, MNRAS, 492, 2161
de Boer T. J. L., Belokurov V., Koposov S. E., 2018, MNRAS, 473, 647

This paper has been typeset from a TEX/LATEX file prepared by the author.